The electrical breakdown of gases by pulsed oscillatory fields

Monk, P. G.

THE ELECTRICAL BREAKDOWN OF GASES BY PULSED OSCILLATORY FIELDS

A thesis submitted to the
University of Durham
for the degree of
Master of Science

P. G. MONK

September 1956 - August 1959

CONTENTS

ACKNOWLEDGMENTS

I would like to record my appreciation to Professor G. D. Rochester for making available research facilities, to the British Electrical and Allied Industries Research Association for their generous financial assistance and to Dr. W. A. Prowse for his patient guidance and advice.

INTRODUCTION

INTRODUCTION

An electron in an electric field is accelerated and thus gains kinetic energy. If its energy is less than Ve electron volts, where Ve refers to the lowest excited state of the gas molecule, the electron can make elastic collisions only. When its energy exceeds this value it can make inelastic collisions in which energy is transferred from the electron to the structure of the molecule and the molecule is then in an excited or ionized state. In a non-ionizing inelastic collision certain distinct atomic states are excited. In a polyatomic molecule for example these may involve rotation and vibration of the molecule.

Provided that an electron has sufficient energy to produce an inelastic collision the probabilities of the occurrence of the various possible collisions are by no means equal. The probability of a particular type of collision occurring may be conveniently expressed as the collision cross section. If there are n particles passing through a gas per second per square centimetre and the mean distance between two collisions is λ , ndx/λ collisions will be made in a distance dx. Assuming that each colliding electron of an electron beam is lost the number lost over a distance dx per second per square centimetre is:

$$dn = -n.dx/\lambda$$

If $n = n_0$ at $x = x_0$ $n = n_0 \exp(-x/\lambda)$ and $1/\lambda = N.Q$

where N is the number of atoms per cubic centimetre and Q is the effective cross section of the atom in square centimetres and is the area of cross section it would have in the collision as a solid sphere on the kinetic theory.

N.Q is the sum of the effective cross sections of all the atoms in one cubic centrimetre of the gas and is called the total effective cross section. It is usually given for a gas at a pressure of 1 mm Hg and at $0^{\circ}C$.

The probability of collision Pc, as used by Brode, Ramsauer, Kollath et al. is defined as the number of collisions made by an electron in travelling 1 cm through a gas at a pressure of 1 mm Hg at a temperature of $0^{\circ}C$. It follows that

$$P_c = 1/\lambda_c = N.Q$$

where λ_c is the electron mean free path.

The effective cross sections Qe and Qi for excitation and ionization respectively are smaller than Q as many collisions occur in which the atom is neither excited nor ionized. The ratio of Qe to Q is termed the probability of excitation at a collision. Similarly the ratio of Qi to Q is termed the probability of ionization at a collision.

In figs. 1 and 2 are shown curves of collision probability Pc, as a function of electron energy for some of the more common substances. For low velocity electrons the potential field of the external electrons is the determining factor for the probability of collision. The similarity of curves for atoms with similar electron arrangements confirms this idea.

In fig. 3 are plotted curves showing probability of ionization at a collision as a function of the energy of the impinging electron.

The energy given to an atom or molecule in an inelastic impact of moderate energy usually affects the outer electron and can conveniently

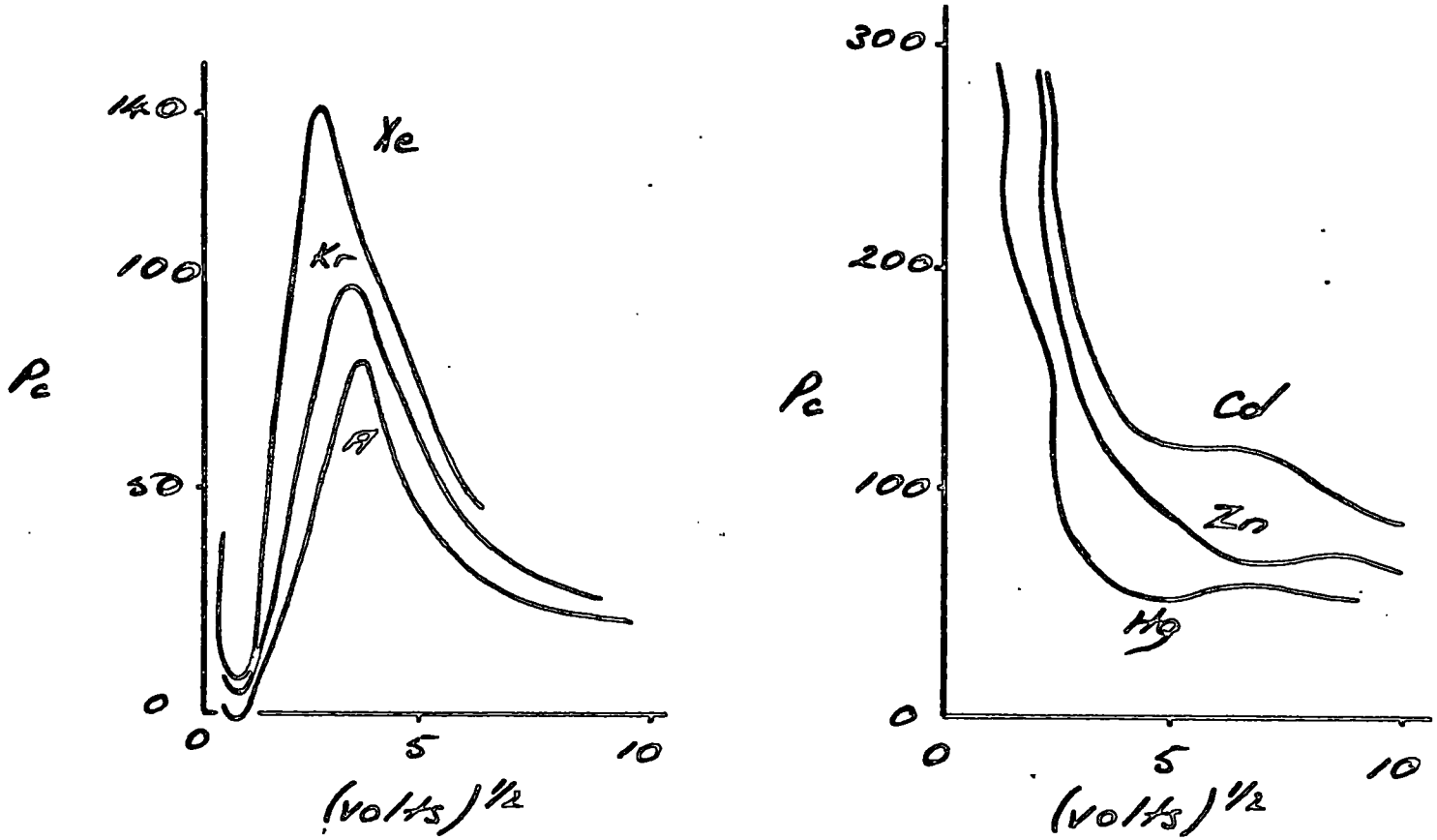

COLLISION PROBABILITY.

Fig 1 of 2

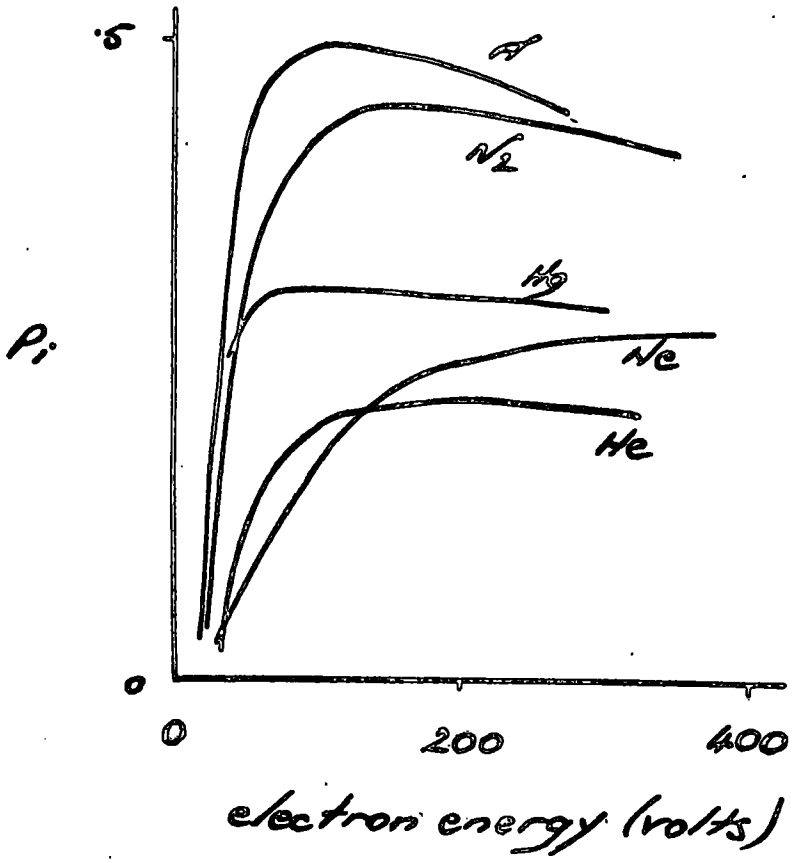

IONIZATION PROBABILITY.

fig 3

be discussed in terms of energy levels. In fig. 4 is shown the energy level diagram for neon. The spectroscopic notation appears beside each level. It will be seen that the ionization energy is 21.5 volts and the lowest excitation level is 16.61 volts. Until the energy of the impinging electron exceeds 16.61 volts all collisions are elastic.

From almost all of the excited states the atom returns to the ground state after a time of the order of 10^{-8} second with an emission of monochromatic radiation. Two of the lower energy states of neon are metastable ($2S_5$ and $2S_3$) and in accordance with the quantum selection rules an atom is unable to return directly from these states to the ground state. These states can exist for up to more than 10^{-1} second and are known to be of considerable importance in breakdown phenomena in unidirection fields.

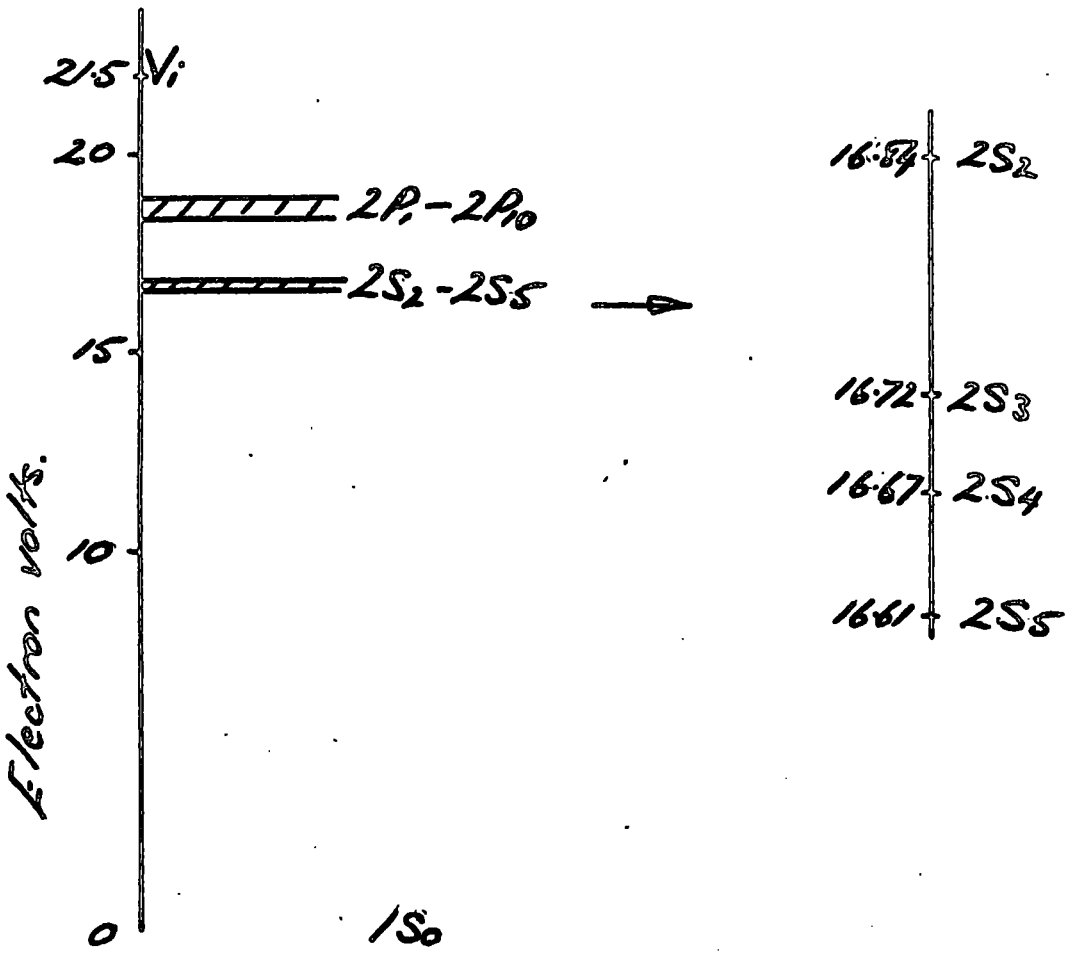

ENERGY LEVEL DIAGRAM FOR NEON

Fig 4.

THE PROBLEM

THE PROBLEM

The problem consists of the measurement of the breakdown time of a gap under certain conditions of breakdown stress, gap width, and gas pressure for various gases.

A rectangular pulse of u.h.f. is applied to a pair of specially profiled electrodes. If the amplitude of the pulse is below the minimum breakdown stress for the particular gap the gap will not break down. If the amplitude of the pulse is above the minimum breakdown stress and the conditions are satisfactory for breakdown the field across the gap will collapse.

The gap is irradiated by ultra-violet light from the breakdown of an auxiliary spark gap. The instant of irradiation is the time from which the timelag to breakdown is measured. Across the test gap there is a pulse of u.h.f., the profile of which is represented in fig. 5. The instant of irradiation can be indicated on the pulse and timelags measured from this point.

The timelag to breakdown of a gap may be separated into two components, (1) the formative and (2) the statistical lag. The formative lag depends upon the nature of the breakdown process and corresponds to the time taken for the discharge to develop across the gap. It is the least time interval between the application of the voltage and breakdown of the gap. The statistical lag depends upon the appearance of an electron in a favourable position in the gap or any other phenomenon of a statistical nature necessary for breakdown.

There are two methods for determining the formative time as a function of the applied voltage:-

(1) a short pulse of duration T is applied to the test gap and the breakdown probability measured as a function of voltage amplitude. The minimum breakdown voltage for the particular value of T is that for which the probability falls to zero.

(2) a long pulse is applied to the test gap and photographic recordings made of the breakdown oscillograms. A statistical analysis of the results is made and the formative time determined for various values of voltage.

APPARATUS

THE APPARATUS

CIRCUITRY

The u.h.f. pulse is produced by rapidly switching on, and after a short delay rapidly switching off an oscillator. The system is shown diagrammatically in fig. 6.

The rectified output from an e.h.t. transformer charges a bank of capacitors constituting the immediate anode supply to the oscillator, held off by a mercury thyratron. As the potential on the capacitor bank rises a fraction of it is fed to a comparator unit so designed that when the input level reaches a predetermined value a negative pulse is fed to the main impulse generator which in turn produces pulses applied as follows:

(1) to the grid of the thyratron, causing the potential on the capacitor bank to be applied to the anode of the oscillator;

(2) via the delay unit to an impulse generator which then produces a large negative pulse which switches off the oscillator after the pre-set delay. The oscillator thus operates for a short time controlled by the delay unit.

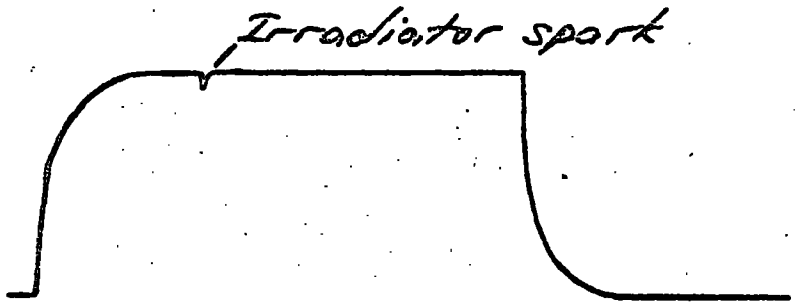

U.H.F PULSE PROFILE fig 5

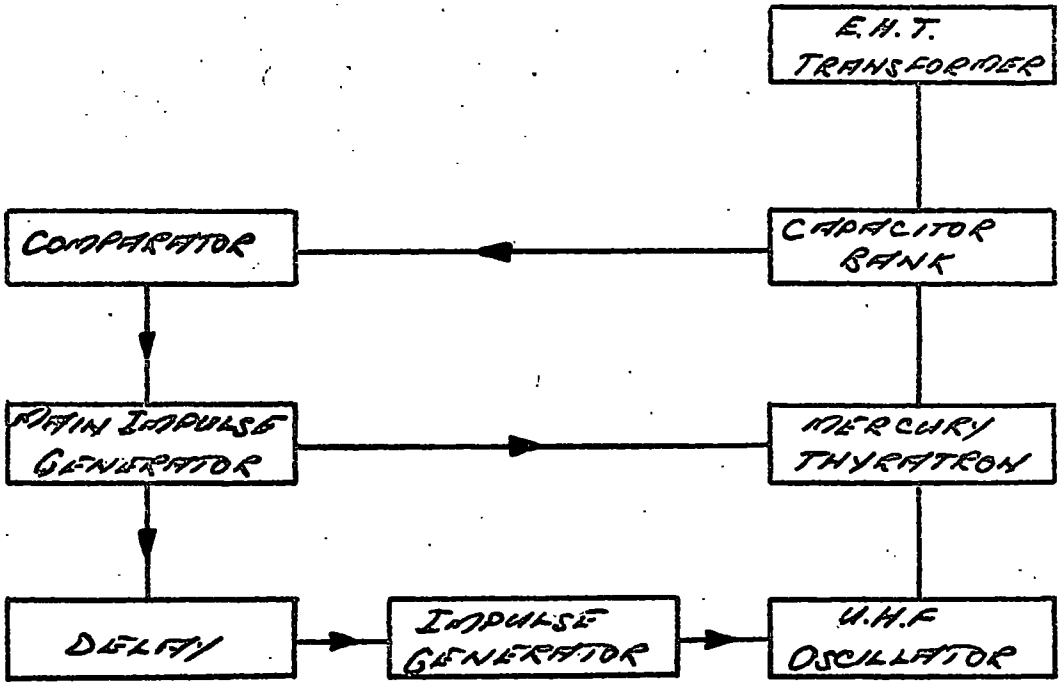

BLOCK DIAGRAM OF APPARATUS fig 6

Operation with pulsed oscillations

Fig. 7 shows the main features of the oscillator designed for the 200 Mc/s region together with a relay device discussed below (p. 8). A tuned-grid, tuned-cathode circuit is employed driven by two triodes in push pull. Parallel cylinders are used as the tuning elements.

Across the bank of capacitors which constitute the anode supply for the oscillator is a potential divider so that a fraction of the potential can be fed to the voltage comparator unit (fig. 8). As the capacitor bank charges a rising positive potential is applied to the grid of the cathode follower buffer stage which is followed by two pentodes constituting a mono-stable trigger circuit. The comparator operates when the potential at the cathode of the triode exceeds that at the cathode of the second pentode. This - the reference potential - is stabilised by a neon tube and can be varied by a potentiometer. Thus the triode is caused to conduct momentarily producing at the anode of the second pentode a negative pulse of amplitude comparable with the local anode supply, which is fed to the grid of an inductively loaded pentode in the main impulse generator.

The pentode (fig. 9) is normally in a conducting state but application of a sharp negative pulse to the grid completely cuts off the current, so producing a large e.m.f., $L\frac{di}{dt}$ of some kilovolts sufficient to fire the auxiliary gap of a trigatron.

A positive pulse from the trigatron is fed via a diode clipper to the main thyratron (fig. 10). When the thyratron fires the capacitor bank is connected to the oscillator.

OSCILLATOR

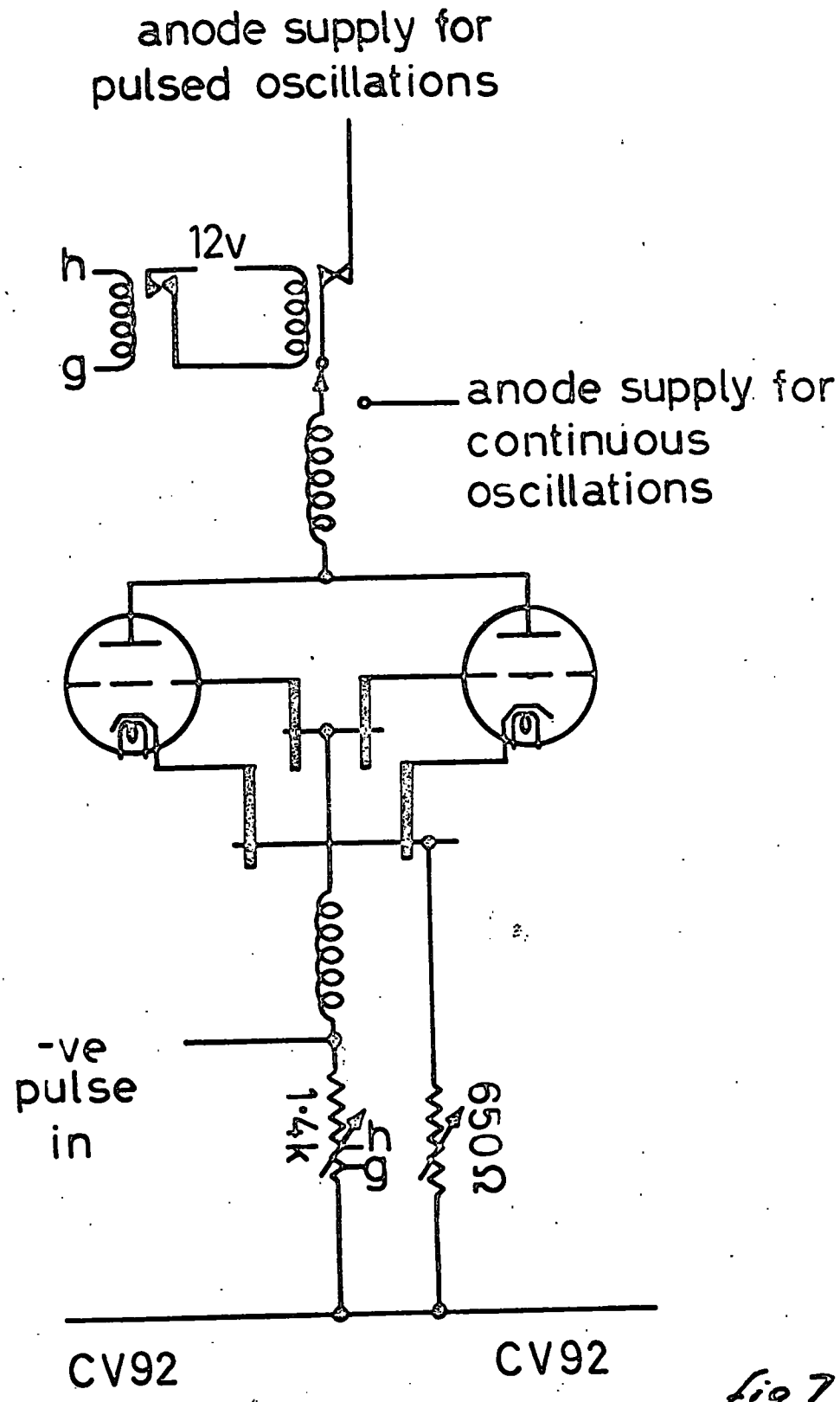

Fig 7

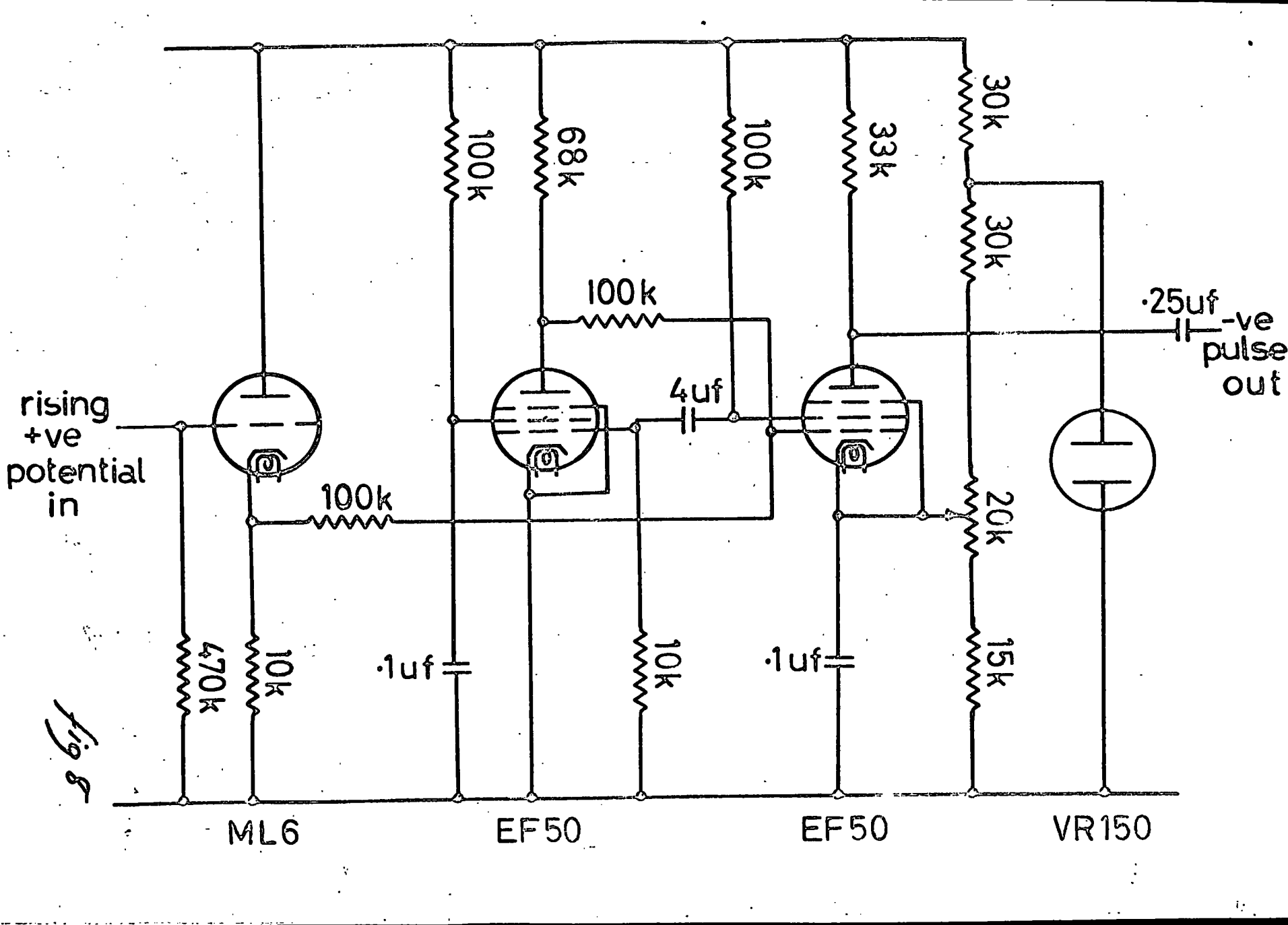
rising
+ve
potential
in
100k
68k
100k
33k
30k
30k
100k
·25uf
-ve
pulse
out
4uf
100k
20k
470k
10k
·1uf
10k
·1uf
15k
ML6
EF50
EF50
VR150

MAIN IMPULSE GENERATOR

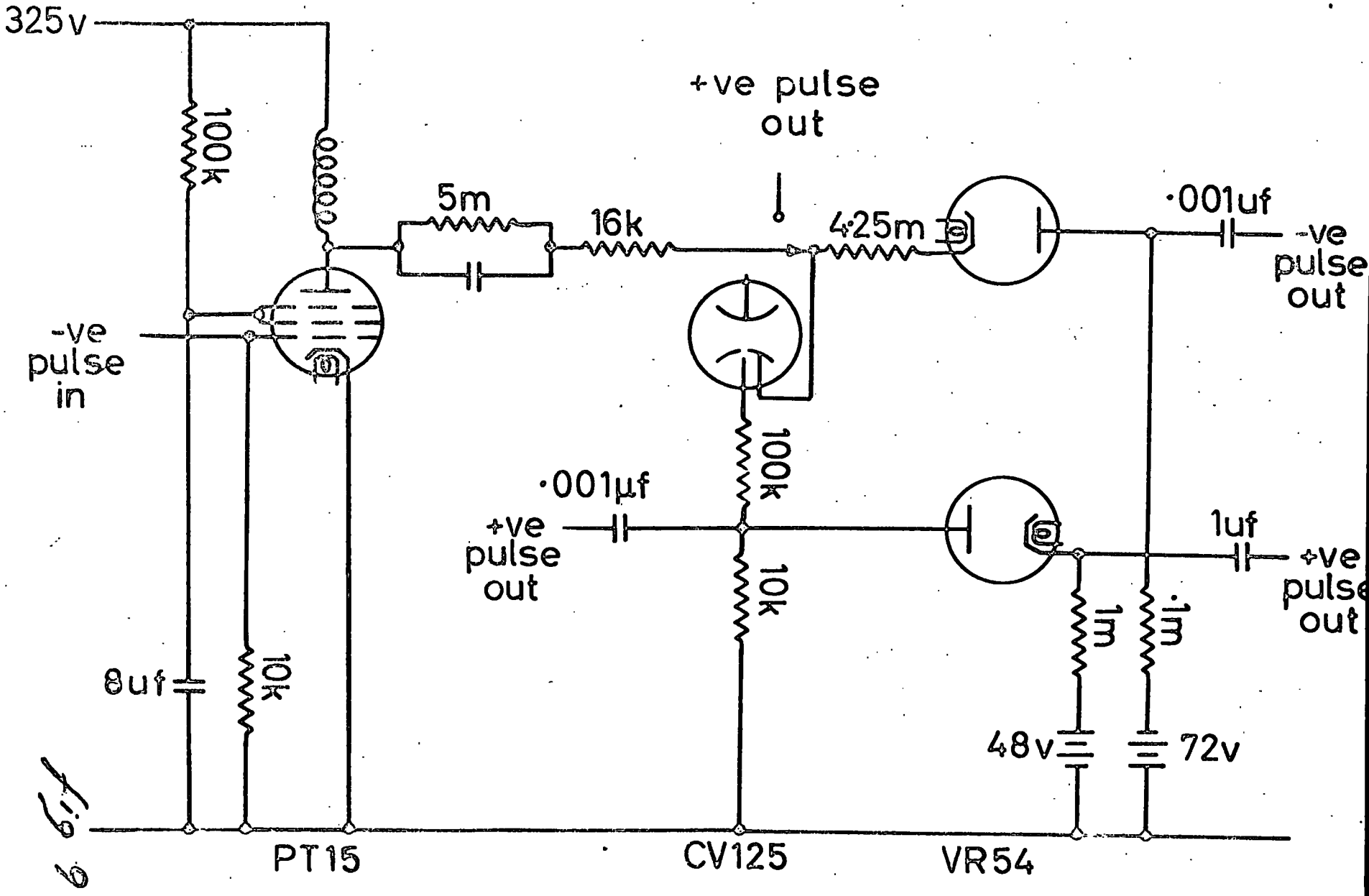

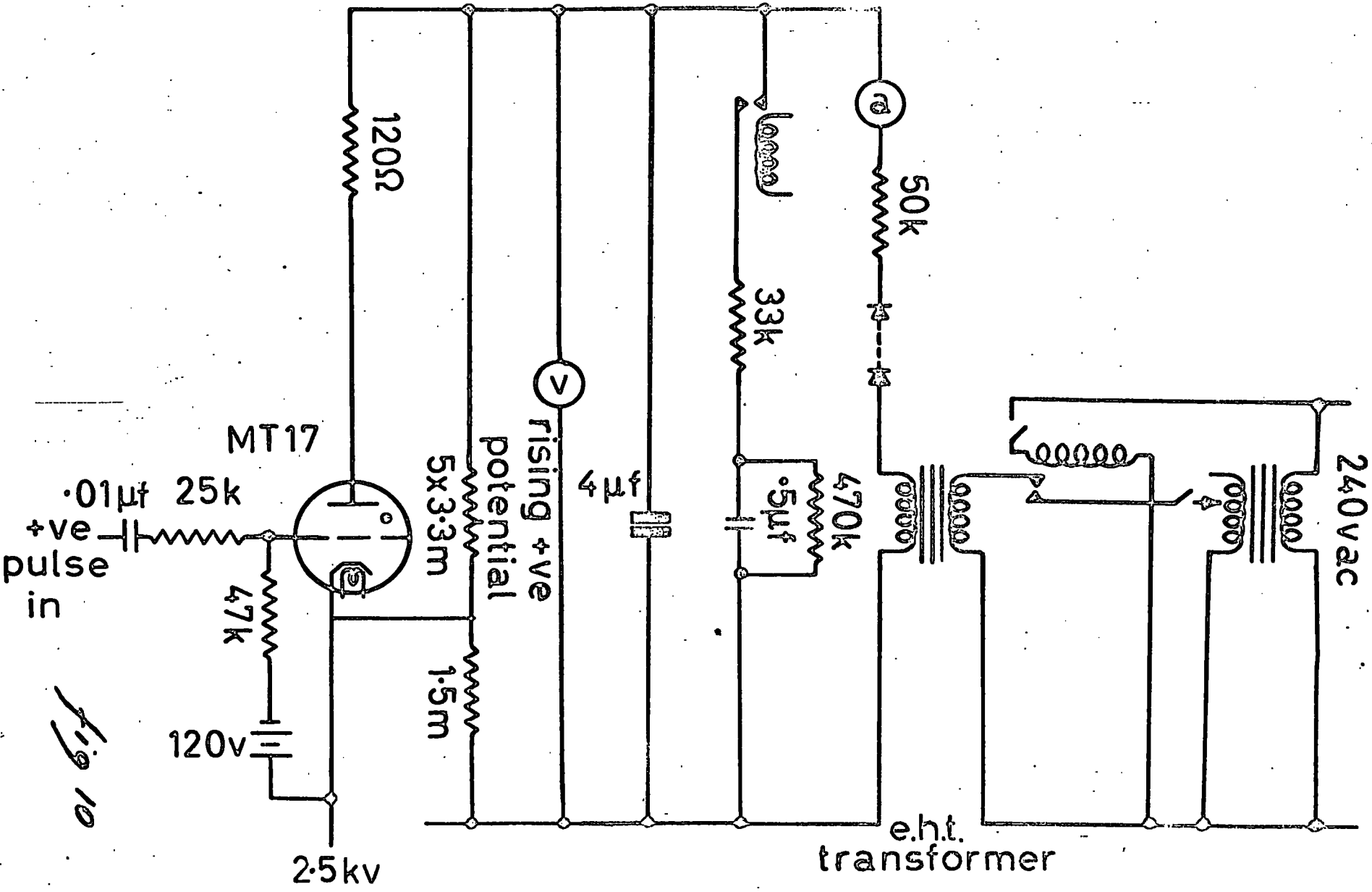
120Ω
MT17
·01µf
25k
+ve
pulse
in
47k
120v
2·5kv
5x3·3m
potential
rising +ve
V
4µf
33k
·5µf
470k
50k
A
1·5m
e.h.t.
transformer
240v ac

Fig 10

The delay unit (fig.11) employs two small thyratrons. The first is fired as a result of the trigatron breakdown the second after a delay determined by the CR combination linking the two valves. C is fixed but regarded as a coarse control and R is continuously variable thus enabling the delay to be varied.

The output from the delay unit is fed to the impulse generator (stop) (fig. 12). The first stage of this is a cathode follower which applies a positive pulse to the grid of a mercury thyratron. The thyratron operates a series of relays which discharge a bank of capacitors through the grid resistor of the oscillator and reset the thyratron by removing the anode potential. The negative pulse from the capacitors to the oscillators grids cuts off the oscillation.

When the oscillator is switched off two relays are operated. One breaks the connection between the thyratron and the oscillator anodes to prevent the thyratron from resuming conduction after application of the pulse to the oscillator grids. The other reduces the charge on the capacitor bank so that the voltage applied to the comparator is below the reference voltage. This is achieved by sharing the remaining charge on the capacitor bank with another capacitor (0.5 μF), the charge on which leaks to earth between the pulses via a bleeder resistor. (fig. 10).

VARIABLE DELAY (PULSE LENGTH)

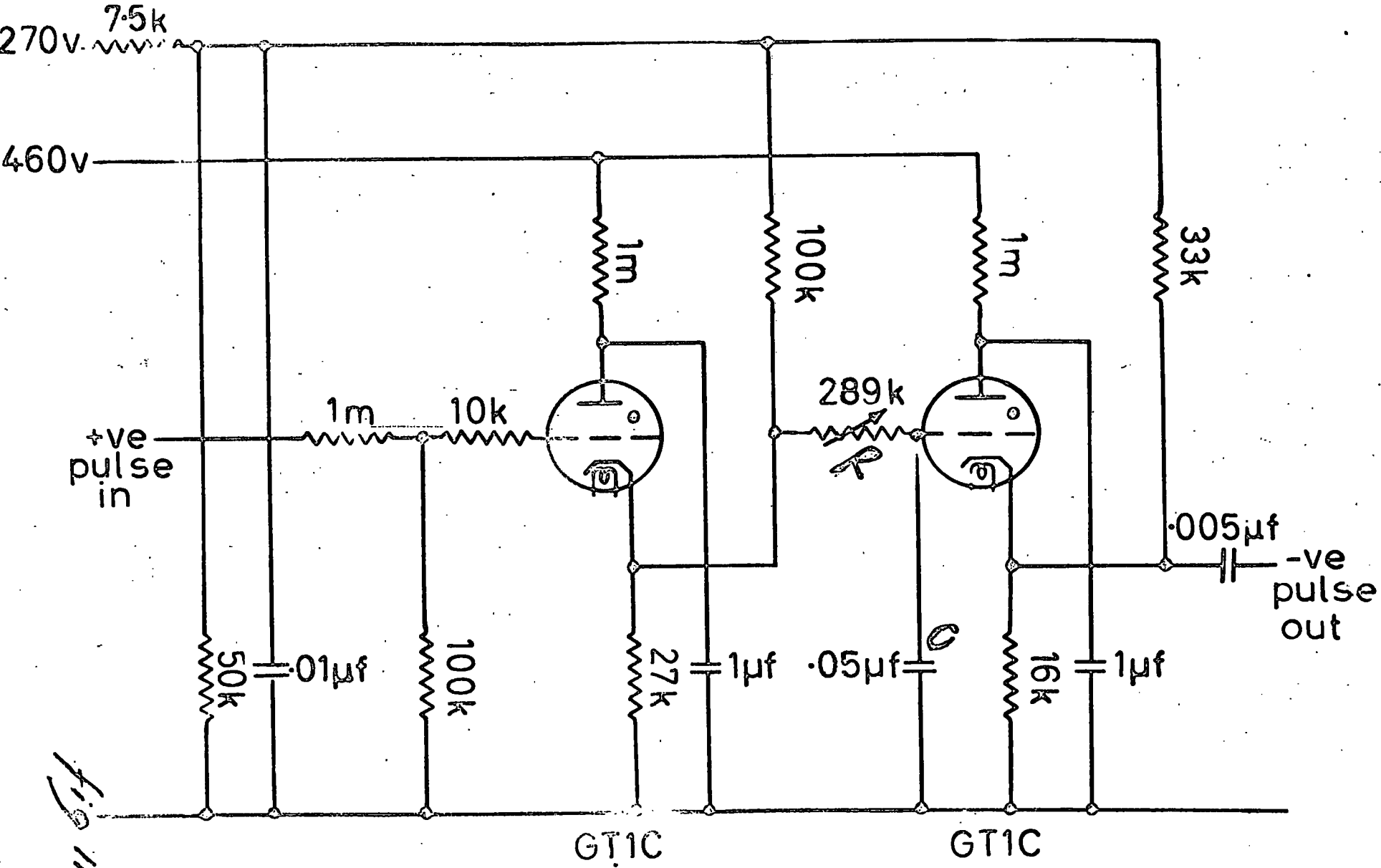

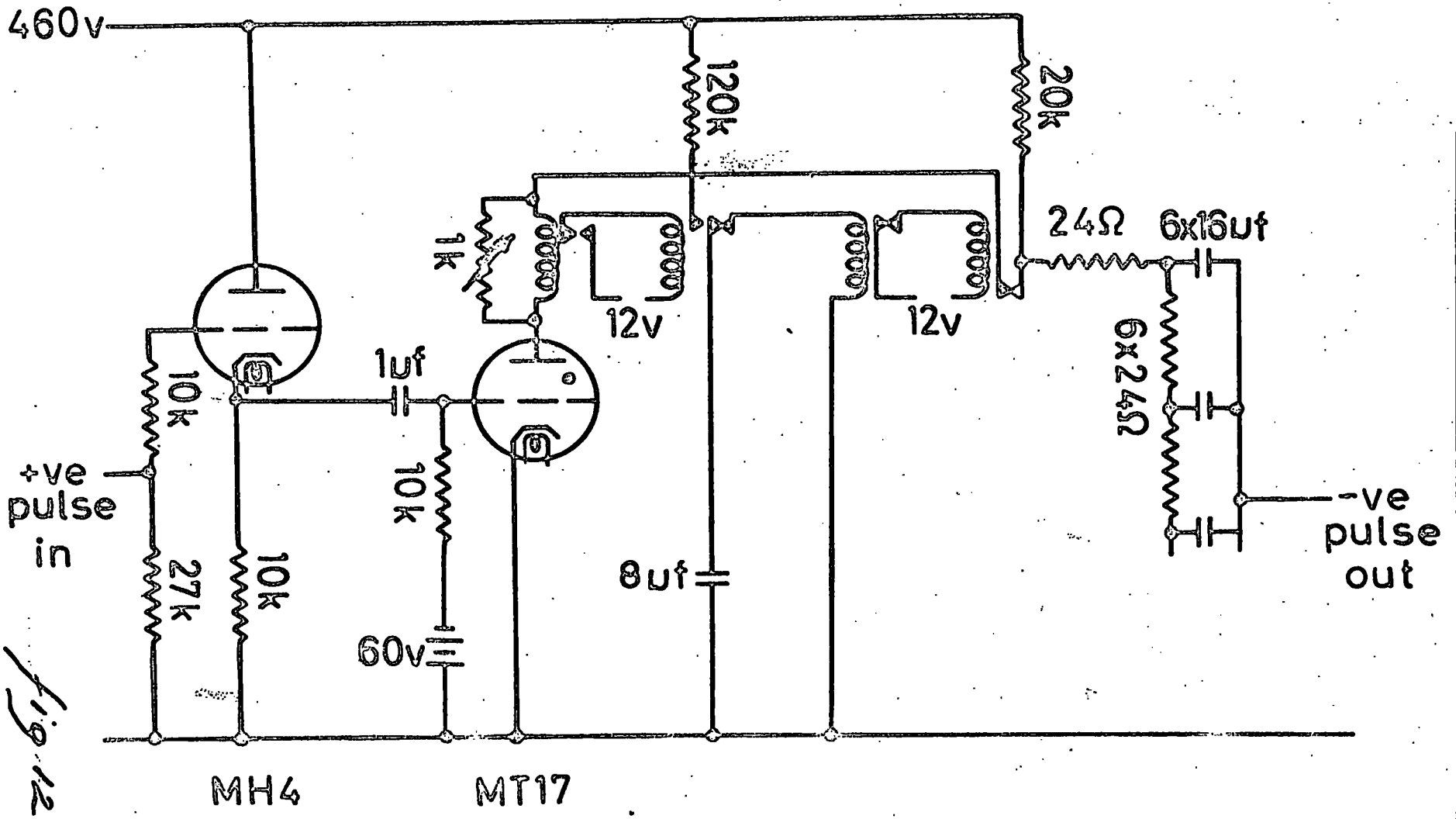
460v
120k
20k
1k
12v
12v
24Ω
6x16μf
6x24Ω
10k
1μf
10k
+ve
pulse
in
27k
10k
10k
60v
8μf
-ve
pulse
out
MH4
MT17

Fig. 12

Operation with sustained oscillations

For calibration and tuning purposes it is required that the oscillator operates continuously instead of intermittently.

For this the anode potential is provided by a rotary converter unit in which the field is provided by current derived from accumulators; continuous variation in output is obtainable by adjusting the series resistor. A household electric light bulb is included in the anode line to act as a resistor and to give a visual indication of the amount of power to the anodes (fig.13).

During operation with sustained oscillations a free-running multivibrator is used to apply a train of pulses to the grid of the inductively loaded pentode, providing several thousand irradiation sparks per second.

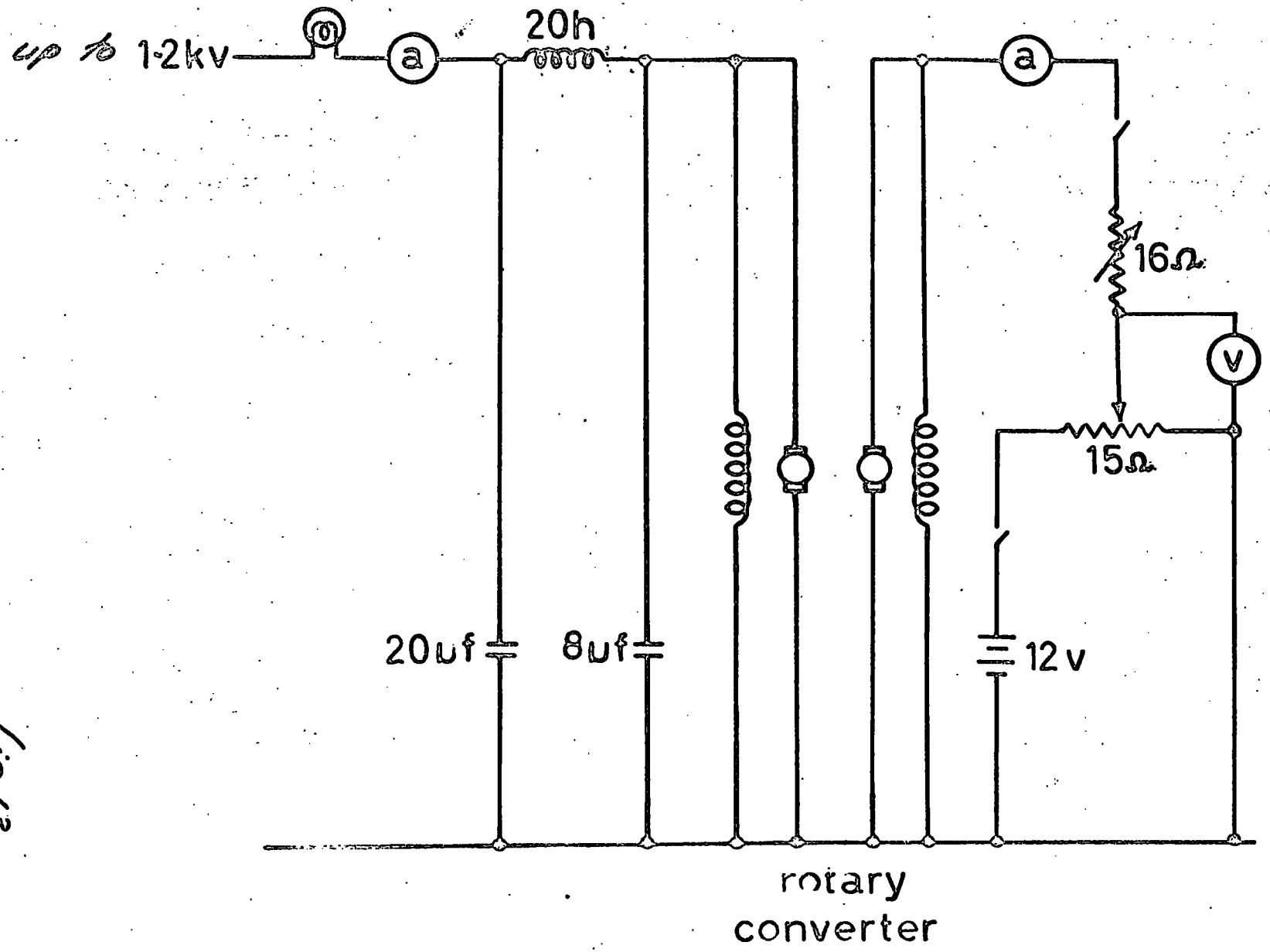

fig 13

BALUNS

The tuned circuits of the oscillator are parallel cylinders but the test gap is situated at the end of a coaxial transmission line.

It is necessary to feed power from a balanced to an unbalanced system. Two methods have been used to couple the oscillator to the coaxial line.

First system - intermediate tuned loop.

The power from the oscillator is picked up by a parallel wire transmission line system. The power from this is fed into the coaxial line by a magnetic loop projecting through a slot in the outer cylinder of the line. (fig. 14).

The amount of power radiated by the parallel transmission line can be indicated roughly by a small neon flash tube (this tended to detune the line slightly) or a 2.5 volt bulb in a tuned LCR circuit.

The transmission line is tuned by successive adjustments of the tuning stub, position of leads to the launching loop and depth of the launching loop in the coaxial line.

Surrounding the launching loop is a quarter wave choke to present a large impedance towards energy flowing over the outer surface of the coaxial line. The coaxial line is tuned by adjusting the position of the tuning piston. The power at the test gap is indicated by an oscilloscope or a galvanometer.

Tuning of the system is very critical and with its several adjustments was found difficult to work. Also little power was appearing at the test gap the reason being possibly because of a bad

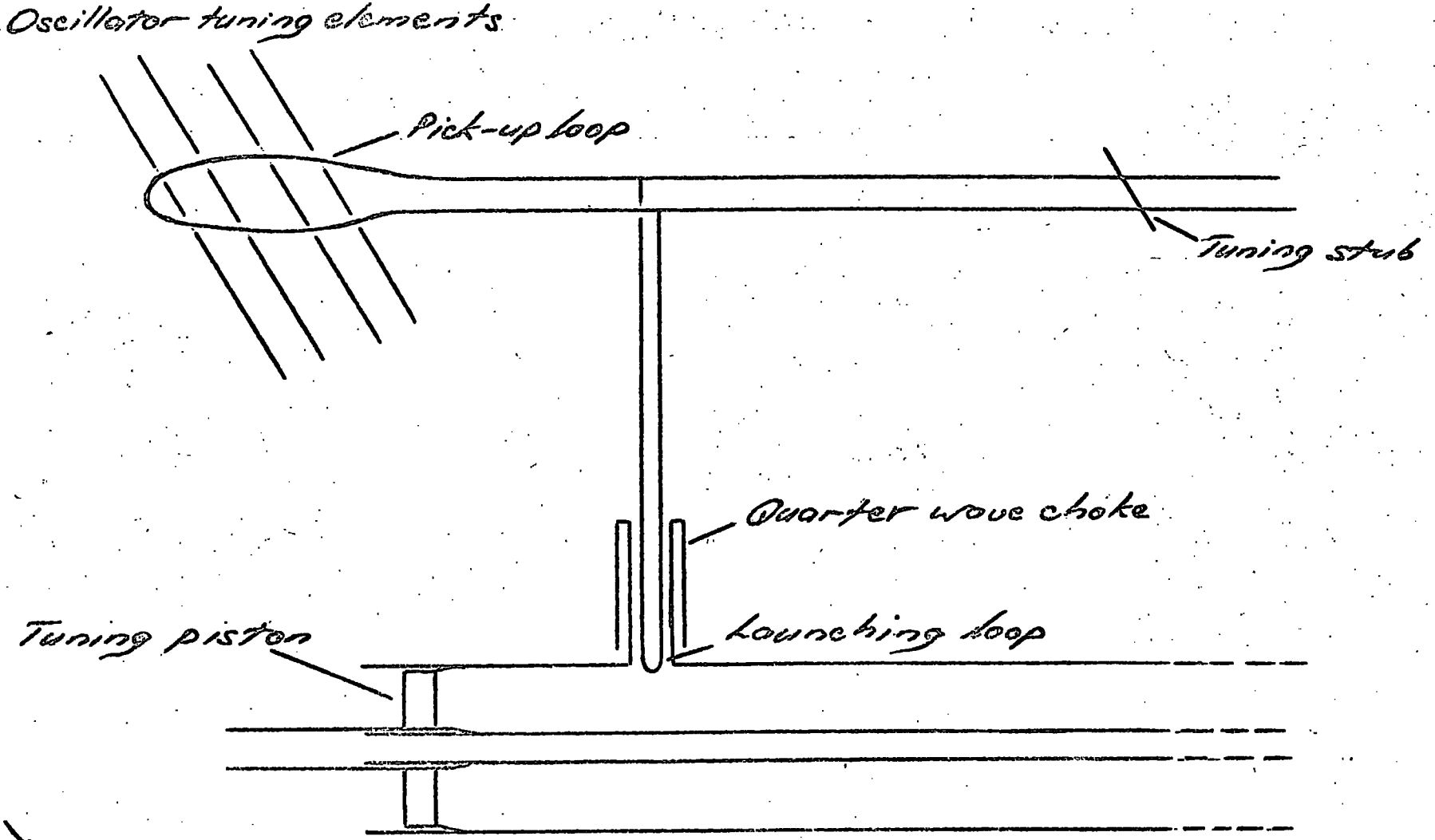

Fig 11

COUPLING BETWEEN OSCILLATOR AND TRANSMISSION LINE.

contact between the tuning piston and the coaxial line. Fig. 15 shows the modification of the tuning piston so that a good contact was ensured at the end of the line and the connection between the sliding and fixed portions of the line was $\lambda/4$ from the end, i.e. at a voltage antinode. This system proved to be no more efficient than its predecessors.

A modification of the parallel transmission line system was considered and two alternative arrangements (fig. 16) were constructed. Neither of these systems made any appreciable increase in the power across the gap or the ease of tuning.

Possible alternatives

The oscillator was then moved nearer to the end of the coaxial line and several more direct systems were considered. (fig. 17).

Systems a and b proved much less efficient than the original system but system c' proved very promising. The line could be tuned by altering the total length of the outer of the coaxial line and also the position of the pick-up loop beyond this. More power than before was appearing at the test gap but a small neon tube in the vicinity of the line indicated that not all the power was going down the inside of the line. A quarter wave sleeve was incorporated to prevent this.

This system shown in fig. 18 was the one finally used and has proved more efficient than its predecessors. Coupling is conveniently varied by bodily moving the oscillator.

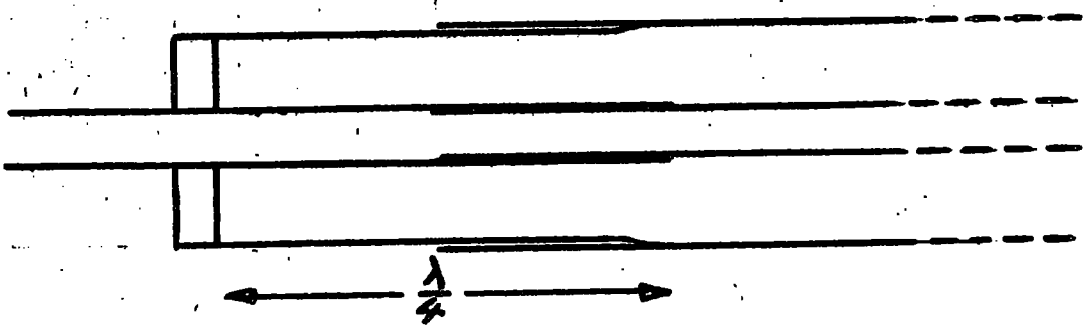

TUNING PISTON fig 15

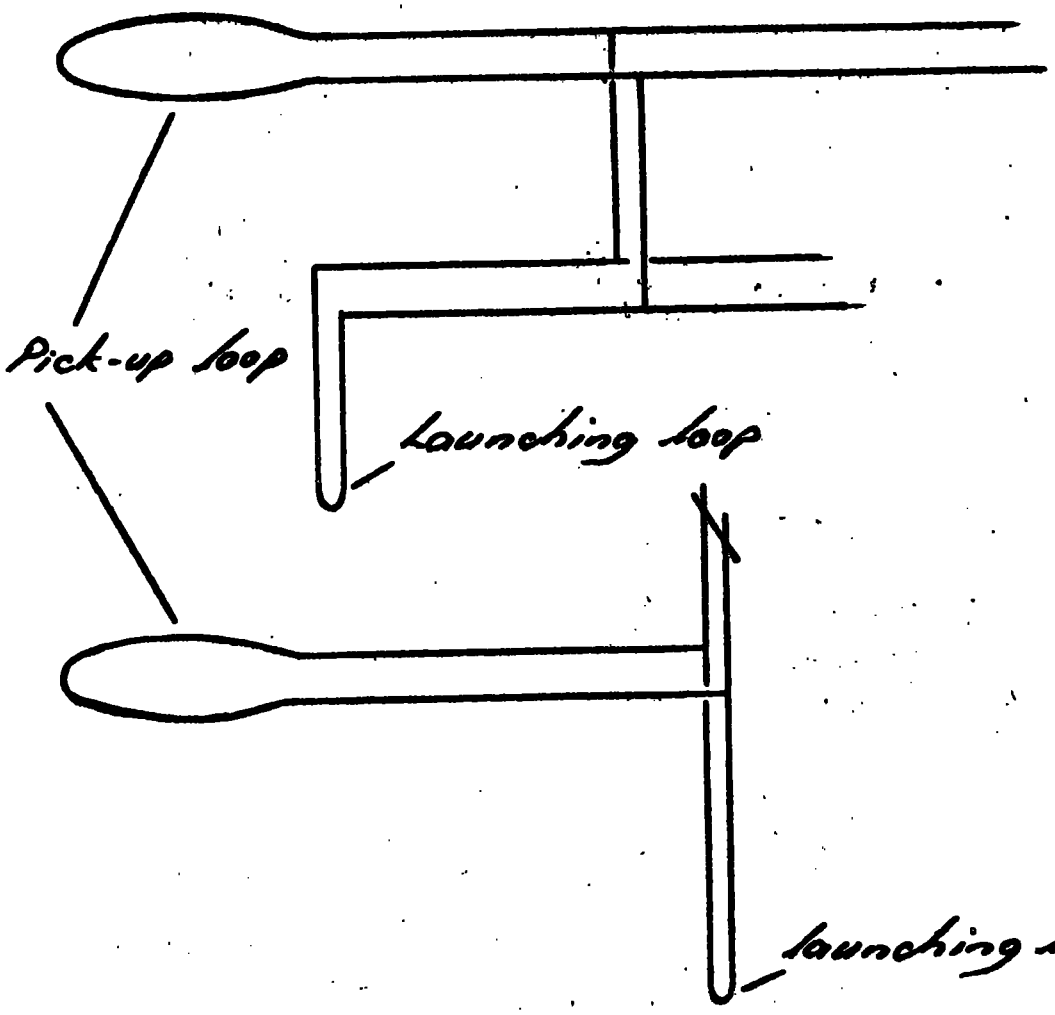

ALTERNATIVE COUPLING SYSTEMS. fig 16

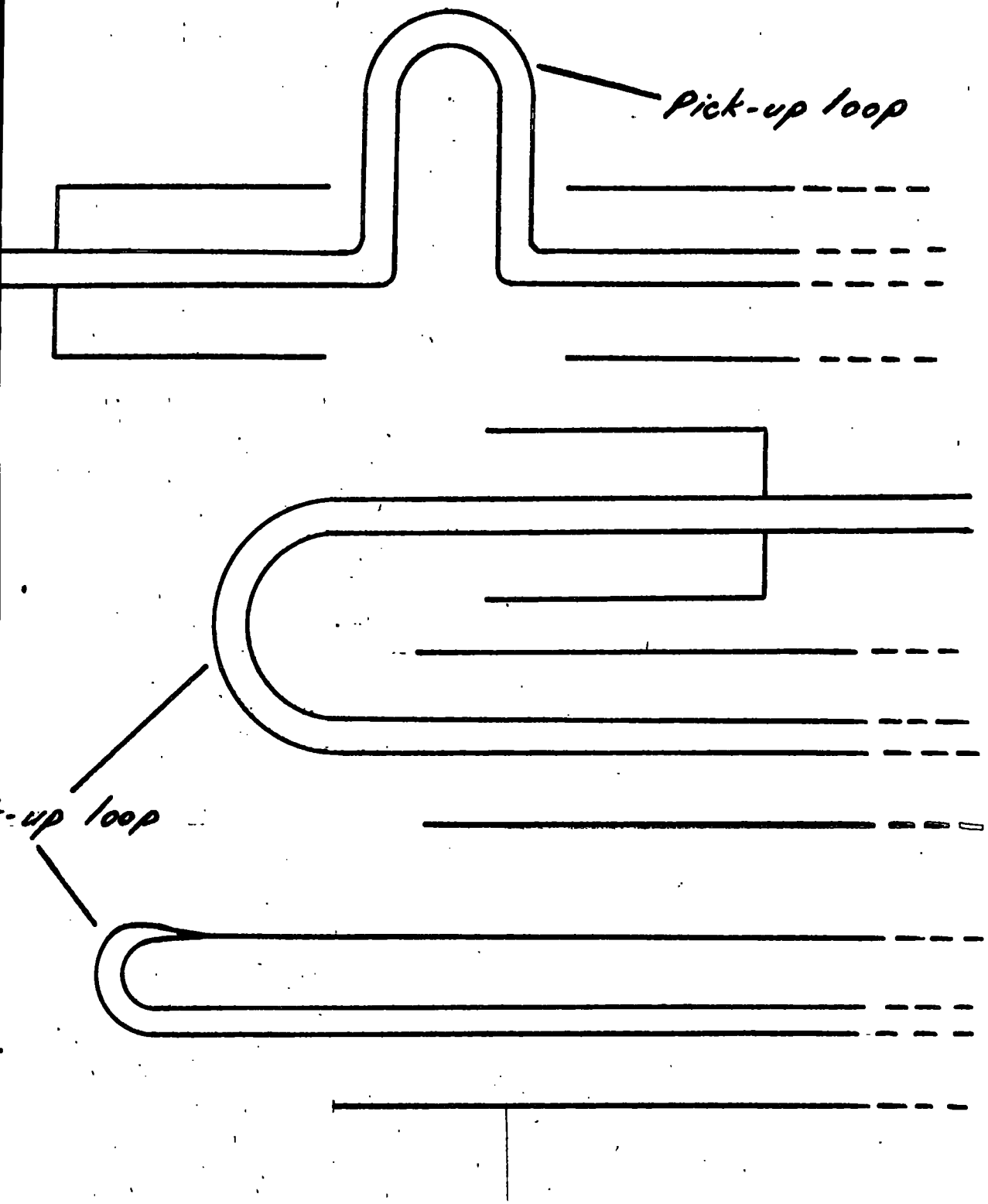

ALTERNATIVE COUPLING SYSTEMS.

fig 17

BALUN

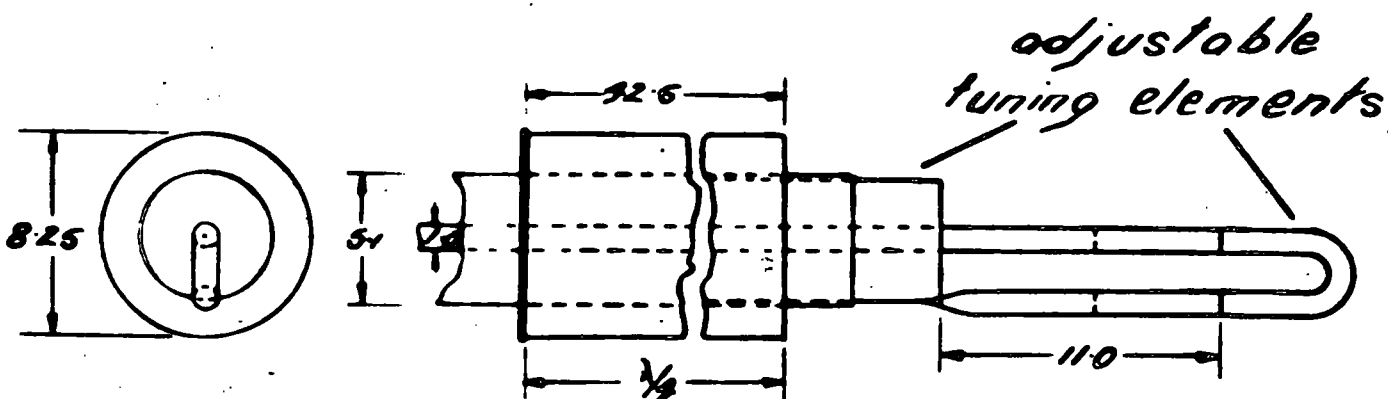

all dimensions in cms. Scale: 1/3 full size

Fig 18

THE TEST GAP

The profile of the u.h.f. pulse applied to the test gap is displayed on an oscilloscope which must be calibrated in terms of the voltage applied to the gap. The difficulty is that the voltage obtainable with pulsed oscillations is higher than the voltage available for calibration with sustained oscillations.

A piston attenuator is included between the end of the coaxial line and the rectifying diode which supplies the oscilloscope. With sustained oscillations the voltage at the end of the line is measured with an electrometer. The piston attenuator is used to apply known fractions of the voltage across the gap to the oscilloscope. Figs. 19 and 20 illustrate the arrangement at the end of the transmission line showing one electrode of the test gap, the electrometer, the launching disc to the piston attenuator and a small tuning capacitor for fine adjustment of the tuning of the line and for changes in tuning when the gap setting is altered.

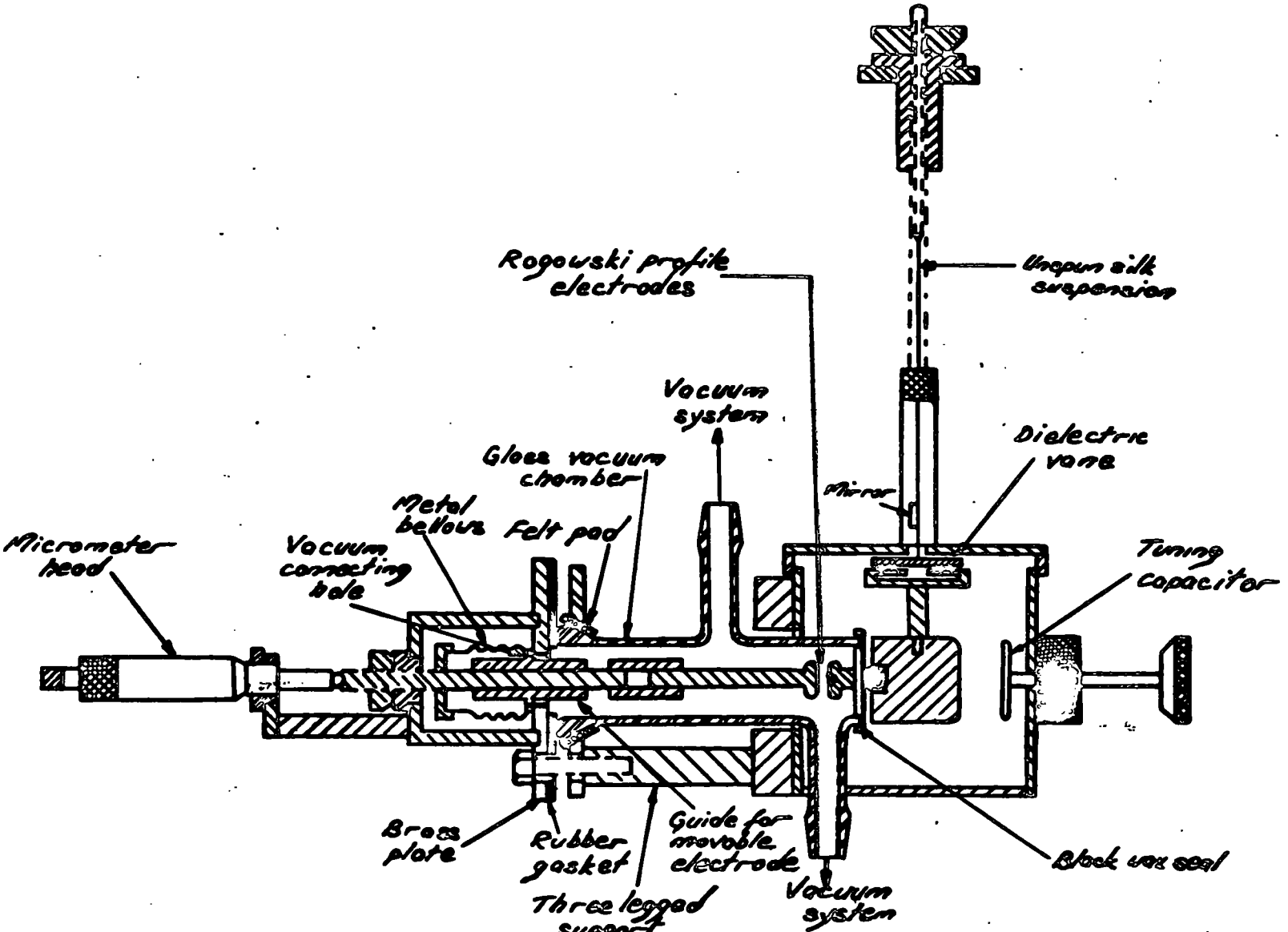

Fig 6

DIELECTRIC VOLTMETER AND SPARK GAP.

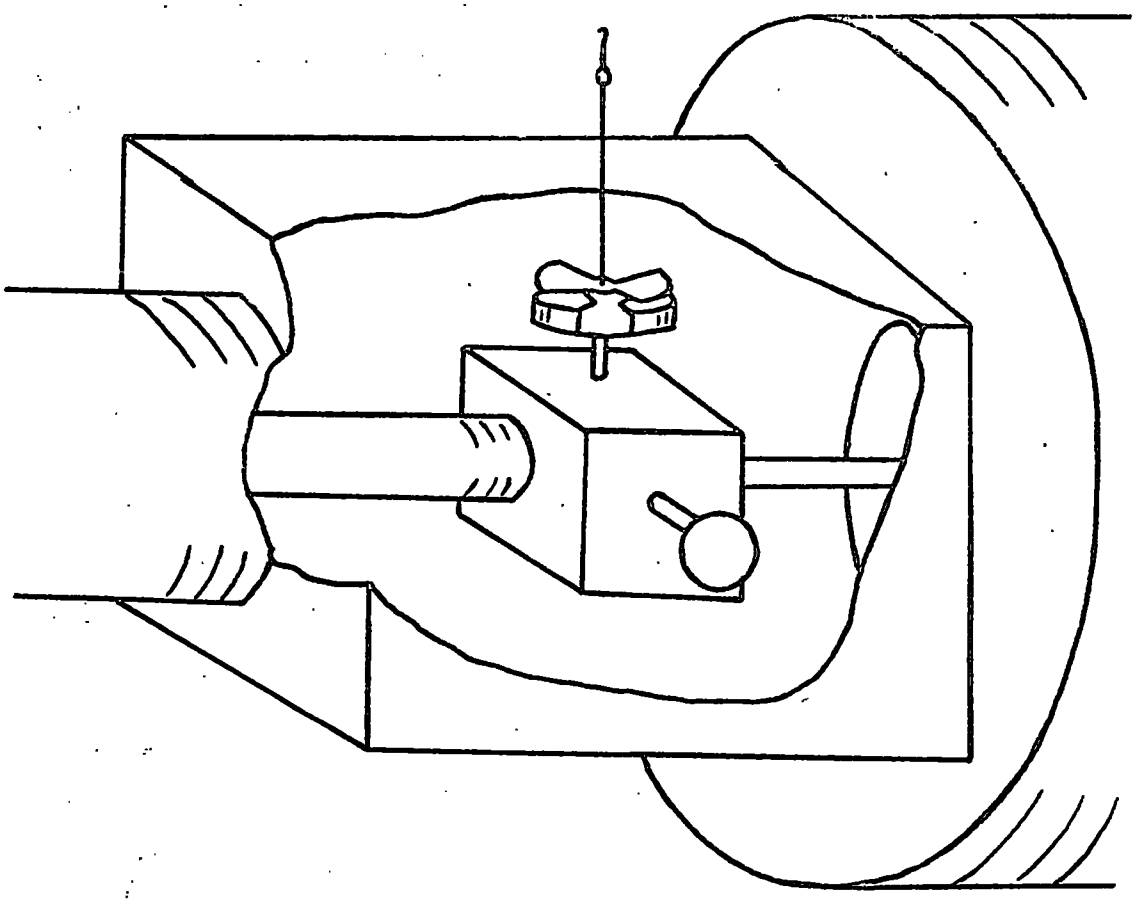

BLOCK AT END OF TRANSMISSION LINE

fig 20

DIELECTRIC VANE ELECTROMETER

Fig. 20 shows the block at the end of the transmission line. The electrometer quadrants are carried on a short pillar, above this is the distrene vane free to rotate about a vertical axis against the constraint of a silk bifilar support.

The deflection varies as the square of the voltage so the instrument is suitable for high frequency measurements provided that the permittivity of distrene can be considered constant. The electrometer is calibrated at power frequencies - the voltage being measured with a sub-standard voltmeter. The calibration curve is shown in fig. 21. The oscilloscope is then calibrated at u.h.f. for one setting of the piston attenuator (fig. 22). From measurement of the gradient of figs. 21 and 22,

voltage at testgap = constant x oscilloscope deflection.

CALIBRATION OF DISTRENG VANE ELECTROMETER AT 50 c/s

fig 21

PISTON ATTENUATOR

The piston attenuator is shown in fig. 23. The cylindrical guide is made from a piece of steel tube, machined inside and copper plated. It carries the launching electrode fixed to the block at the end of the coaxial line and a surrounding ring fixed to a polystyrene support. The pick-up disc and ring also carry the diode rectifier and associated load resistor from which the output is taken to the oscilloscope.

For a cylindrical attenuator the attenuation constant is given by

$$\alpha = 2\pi\left(\frac{1}{\lambda_c^2} - \frac{1}{\lambda^2}\right)^{\frac{1}{2}}$$

where λ_c is the cut-off wavelength and λ is the free space wavelength of the oscillation.

If V_1 and V_2 are the voltages at the pick-up disc for settings of the piston Z_1 and Z_2

$$\log \frac{V_1}{V_2} = \alpha(Z_1 - Z_2)$$

from which by calculation $\frac{\Delta \log V}{\Delta Z} = .133.\ cm^{-1}$

The value of $\frac{\Delta \log V}{\Delta Z}$ was determined experimentally from a series of observations of distrene vane deflection, oscilloscope deflection and piston attenuator setting. The mean experimental value was $0.138\ cm^{-1}$.

The gain of the oscilloscope and the setting of the piston attenuator are adjusted so that the voltage by sustained oscillations produces a convenient deflection on the oscilloscope. When pulses are used the voltage amplitude is much greater than this and the attenuator is altered to a new value giving a convenient deflection.

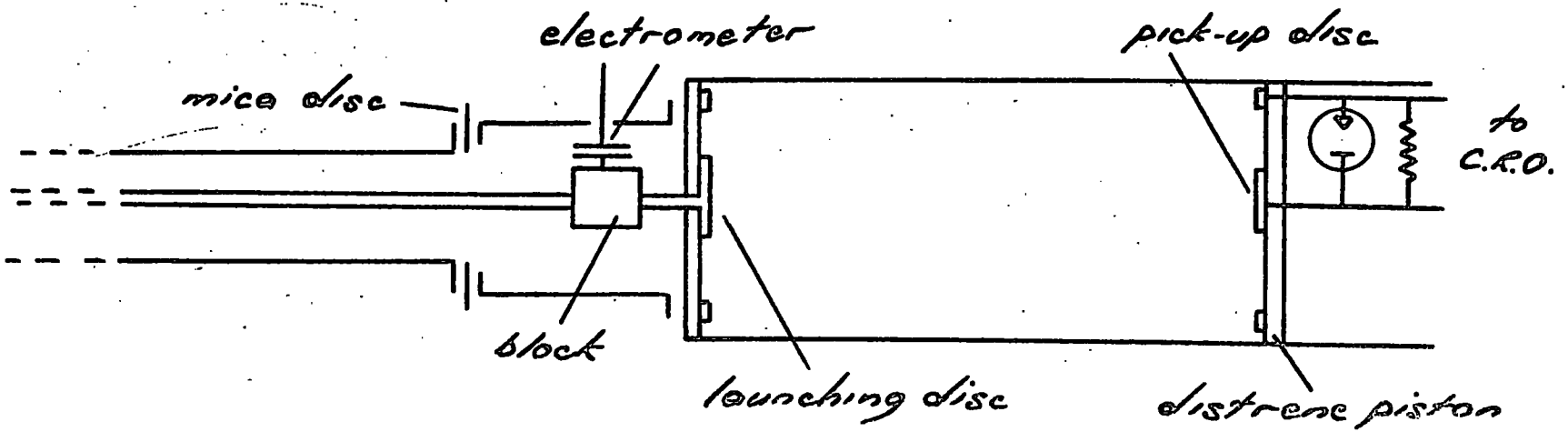

CROSS-SECTION ALONG THE TRANSMISSION LINE.
BLOCK AND PISTON ATTENUATOR.

IRRADIATION OF THE TEST GAP

If the voltage across a gap is increased in small steps it is observed that the gap will only break down if the voltage exceeds a certain minimum value. For a particular voltage above this value the time between application of voltage and onset of breakdown is subject to statistical fluctuations. One probable cause of these fluctuations is the time taken for a casual electron to appear in a part of the gap where it can lead to a series of events which finally cause instability and breakdown.

It has been known for a long time that irradiation of the gap considerably reduces the statistical lag. Instead of waiting for a casual electron from natural sources (e.g. cosmic rays) electrons may be put into the gap by irradiating with ultra-violet light, X-rays or by placing a small radioactive source near the gap.

Rowbotham, in his preliminary experiments on neon, used a small radioactive source near the test gap but this has since been replaced by an ultra-violet source consisting of a small auxiliary spark gap situated at approximately 35 cm from the test gap. Experiments were performed by Prowse and Lane on the effect of the distance of the irradiator from the test gap on the breakdown stress. They found that as the irradiator was brought near to the test gap the breakdown stress was reduced slightly. From their results it would appear that the irradiator spark at 35 cm from the test gap will not affect the breakdown stress.

The advantages of using the present system instead of a radioactive source are:

(1) the initial electrons can be put into the gap after the pulse across the gap has risen to its maximum value; this ensures that for large overvoltages the gap does not breakdown while the voltage is still rising;

(2) the instant of irradiation gives a zero from which measurements of timelag to breakdown can be made;

(3) the ultra-violet light from the spark can easily be collimated into a narrow beam so that it is not incident upon the electrodes of the test gap but produces electrons only in the body of the gap.

The breakdown of the irradiator is initiated by a pulse from the main impulse generator. The pulse is delayed so that irradiation is not produced in the gap until the u.h.f. pulse has risen to its maximum value.

The irradiator delay unit (fig. 24) is similar to the unit which delays the cut-off pulse to the oscillator. The output from the delay unit is fed to the grid of an inductively loaded pentode causing at the anode a large e.m.f. which is fed via a coaxial cable to the irradiator spark gap.

Originally the high voltage pulse was capacitively applied to the electrodes of the irradiator via external sleeves concentric with the electrodes (fig. 25a). With this system the magnitude of the spark fluctuated considerably. This was probably due to charge building up on the glass walls of the tube supporting the irradiator.

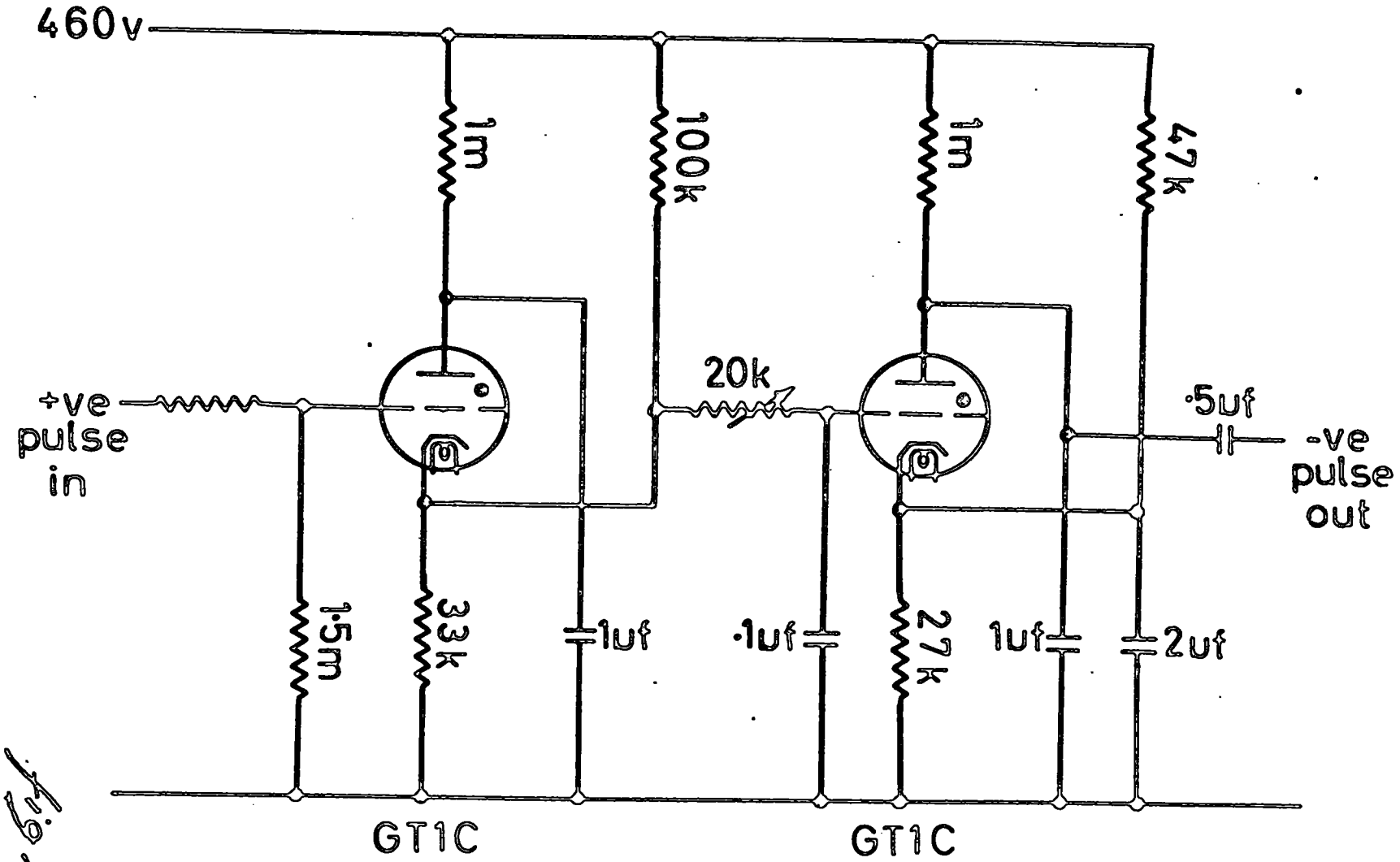
460v
1m
100k
1m
47k
+ve
pulse
in
20k
·5uf
-ve
pulse
out
1·5m
33k
1uf
·1uf
27k
1uf
2uf
GT1C
GT1C

Fig 24

In the present system direct contact between the spark gap and the spark generator is made by using metal-glass seals (fig. 25b). Provision is made so that at very low pressures the size of the irradiator spark can be reduced. If this is not done breakdown of the irradiator gap will ionize the gas in the test gap. This system has proved more efficient than its predecessor and results have been more consistent since using it.

Two collimating apertures are used in the system to restrict the radiation. Of these the lower is a constriction in the glass tubing and the upper is made of metal with a hole in the centre. Both are provided with a by-pass to avoid stagnation of the gas in the system.

VACUUM SYSTEM

The requirements of the vacuum system are:

(1) it can be used with various gases;

(2) the pressure can be varied by small amounts;

(3) the pressure can be measured accurately.

The system is shown diagrammatically in fig. 26. It is built of 1, 1.5 and 2 cm Pyrex tubing. The gas used is spectrally pure and is supplied in 1 litre flasks. A pipette system is incorporated between the gas supply and the main vacuum system to enable the pressure to be adjusted by small amounts. This ensures that any pressure can be obtained accurately and repeated if necessary.

The discharge chamber (fig. 19) in which are situated the test electrodes, is constructed from 1 inch standard Pyrex pipeline. It is approximately 10 cm long with two outlets. One end of the chamber is ground flat and is sealed with black wax to the metal plate carrying the electrode at the end of the inner conductor of the transmission line. The other end is sealed by a rubber gasket clamped tightly between the end of the chamber and a brass plate carrying the other electrode and micrometer head for measuring the width of the test gap.

Four pressure gauges are used in the system: Bourdon gauge, thermal (Pirani) gauge, differential manometer and mercury manometer.

The Bourdon gauge has a range of 0-20 mm Hg and is useful as an indicating rather than a measuring instrument.

The Pirani gauge is to indicate the low pressures encountered when pumping out. It is also useful for detecting leaks and dry taps by the hydrogen Pirani technique.

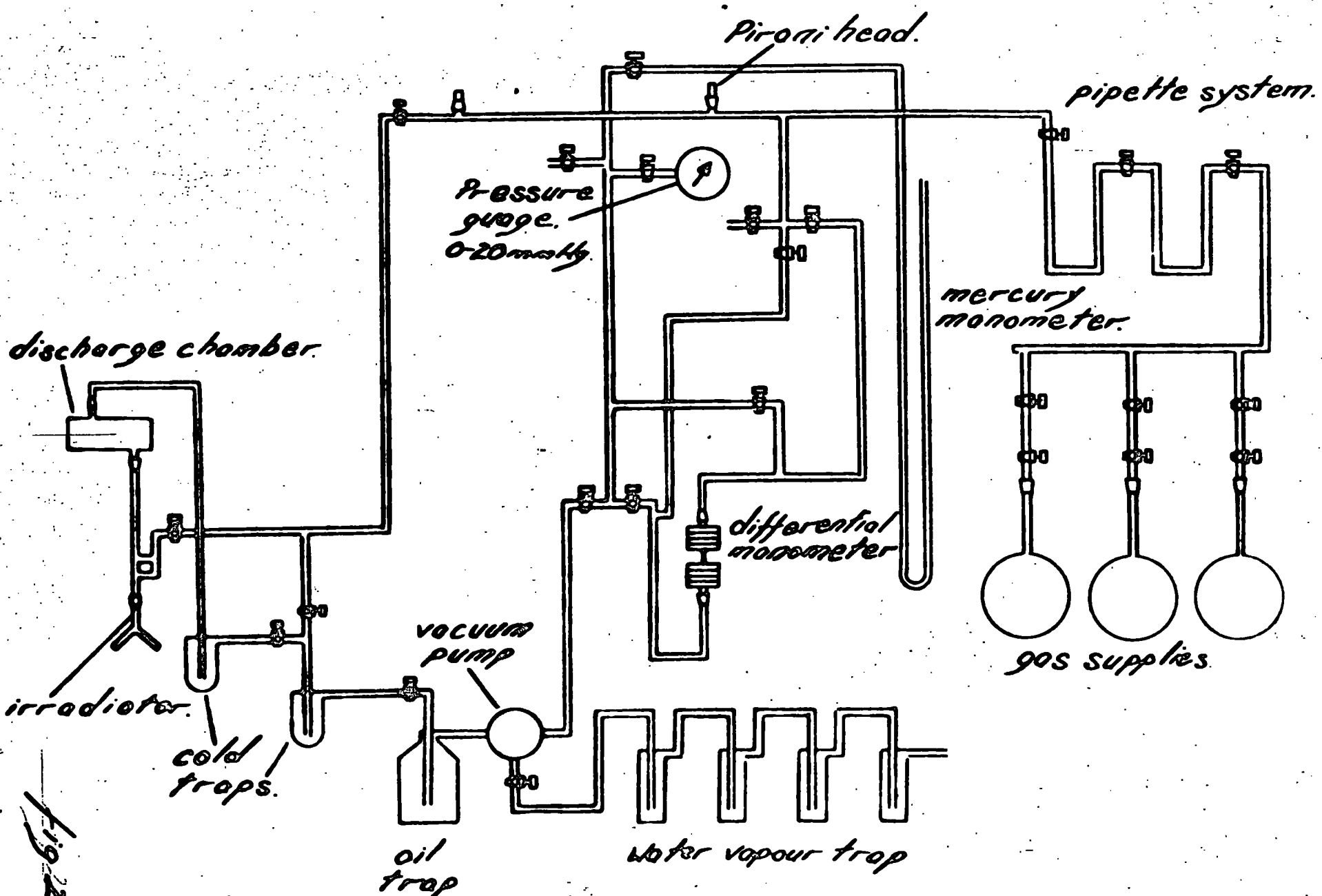
Pirani head.
pipette system.
Pressure guage. 0-20 mm Hg.
mercury manometer.
discharge chamber.
differential manometer
vacuum pump
irradiator.
cold traps.
gas supplies.
oil trap
water vapour trap

Fig 226

The mercury manometer is the reference against which the Bourdon gauge and the differential manometer are calibrated. Except during calibration the mercury manometer is isolated from the rest of the system (and at all times is isolated from the main part of the system) to avoid contamination of the electrodes and the gas under investigation.

The differential manometer is shown in fig. 27. It consists of two opposed stacks of ten capsules with reinforced rims (as used in aneroid barographs) joined by a screwed rod to which is fixed a platform supporting an optical lever system for magnification of the deflection of the bellows.

The lower side of the differential manometer is pumped hard and the upper side connected to the mercury manometer. For various pressures the deflection of the differential manometer can be determined as a function of the height of the mercury column. The calibration curve is shown in fig. 28 and has remained constant over a series of calibrations during a period of two years.

For the relatively high gas pressures it was intended to use it was felt sufficient to use only a backing pump and to rely on repeated flushing of the apparatus to achieve the required purity of the gas in the system, particularly as baking out was not practicable.

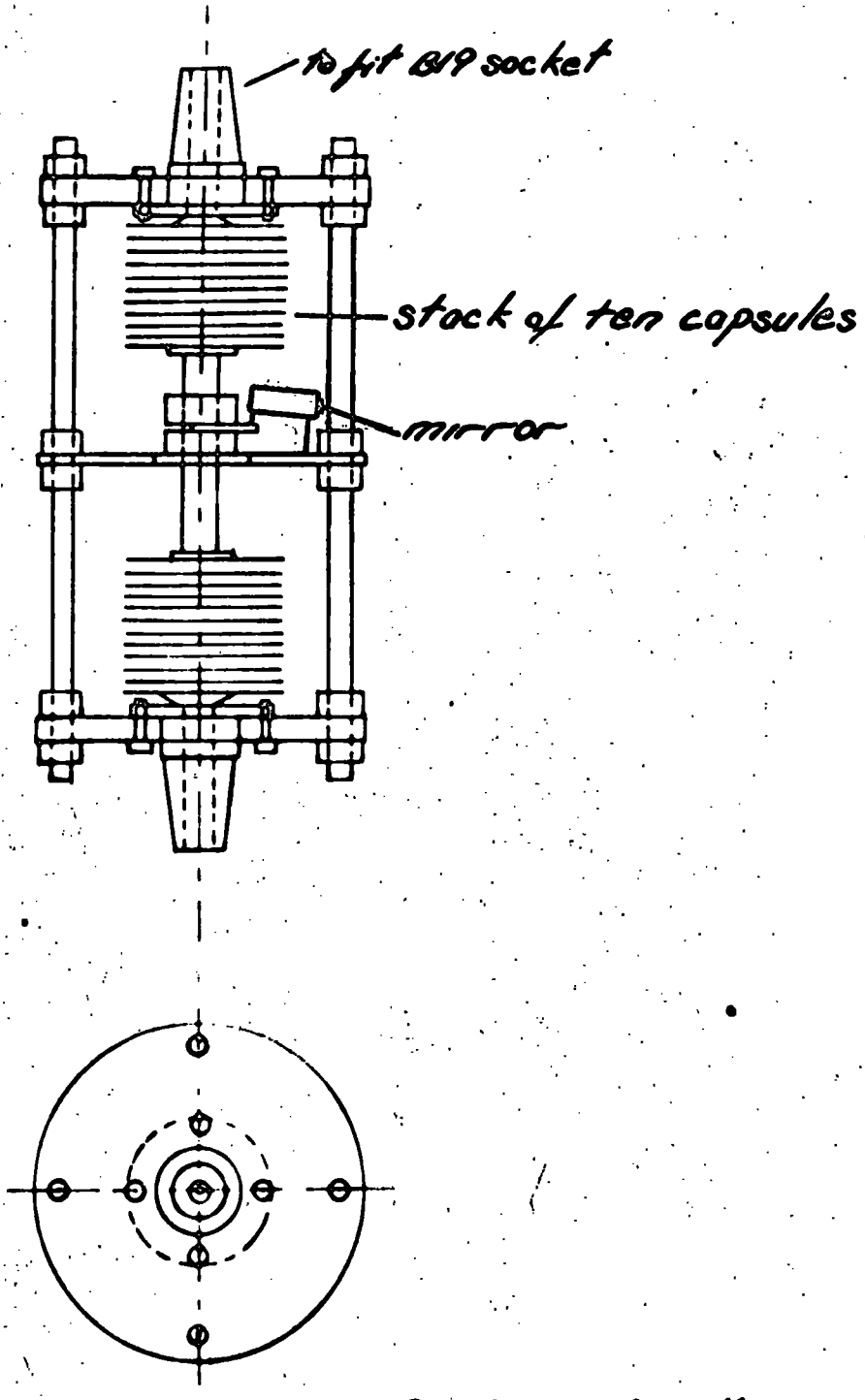

Scale: half full size

DIFFERENTIAL MANOMETER fig 27

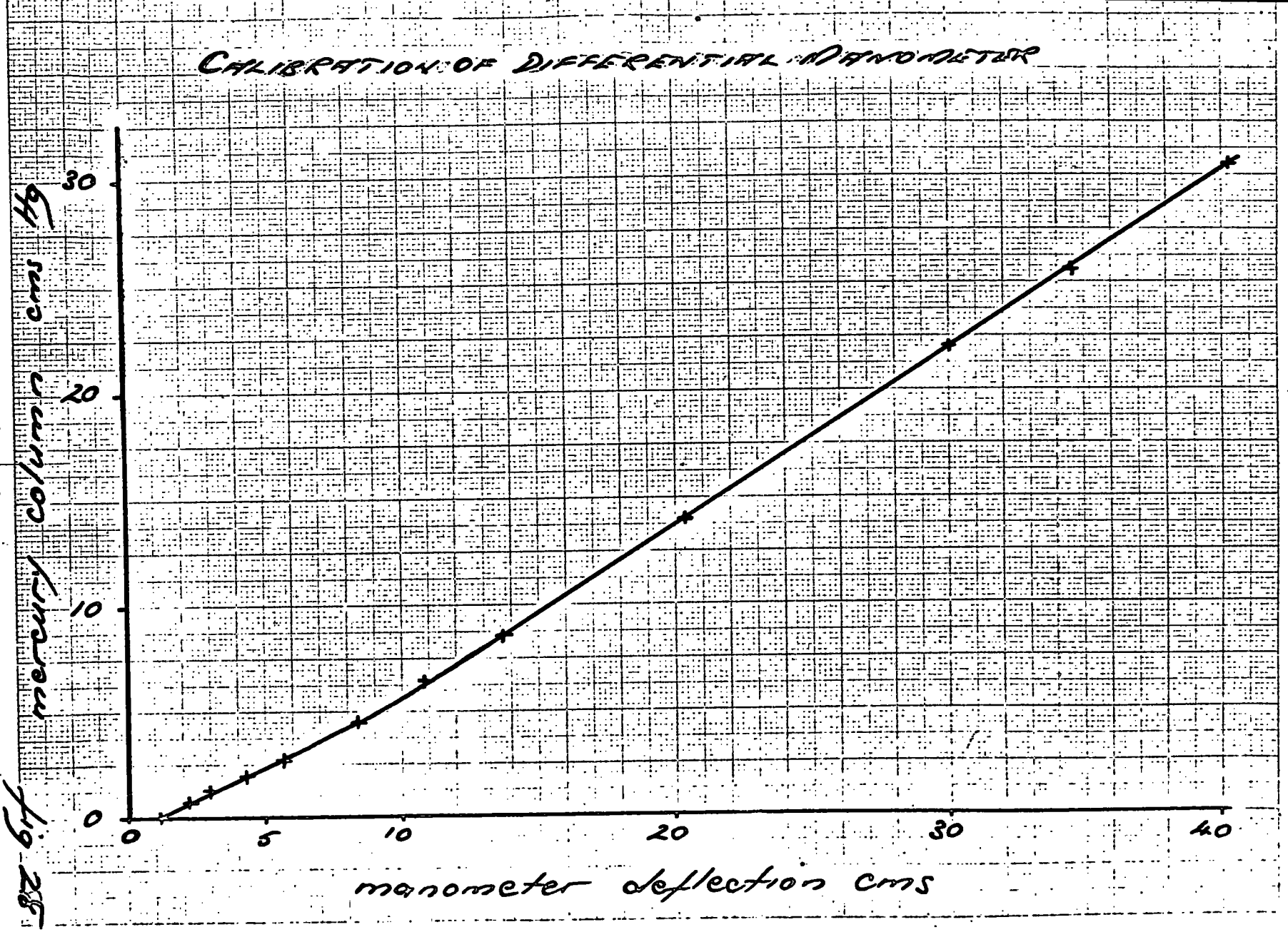
CALIBRATION OF DIFFERENTIAL MANOMETER
Hg column in cms
0
10
20
30
0
5
10
20
30
40
manometer deflection cms

Fig. 28

RECORDING OF RESULTS

RECORDING OF RESULTS

For breakdown events involving no observable timelag to breakdown observations were made visually but other breakdown events were recorded photographically.

Visual

These results could either be obtained by observing the test gap or the breakdown oscillograms. The latter was more suitable as occasional timelags would be noticed.

Photographic

The oscilloscope can be fitted with a single shot camera with a wide aperture lens. The camera is supplied with 12 feet capacity 35 mm Ilford H.P.3 film. The apparatus is adjusted to operate at about one pulse per second and the film moved on between pulses.

Typical traces are shown in fig. 29; a shows a pulse with no breakdown, b shows the same pulse with irradiator mark and breakdown, c is the same as b but using a faster sweep.

Initially several hundred pulses were photographed with no breakdown in the gap. Measurements of pulse height were then made to ensure that this was consistent for the duration of the observations. Calibration traces from a substandard oscillator were also photographed to give an accurate timescale to the pulses.

For actual measurements pulses like fig. 29c were photographed. On each recorded pulse, measurement was taken of pulse height h, and pulse duration t.

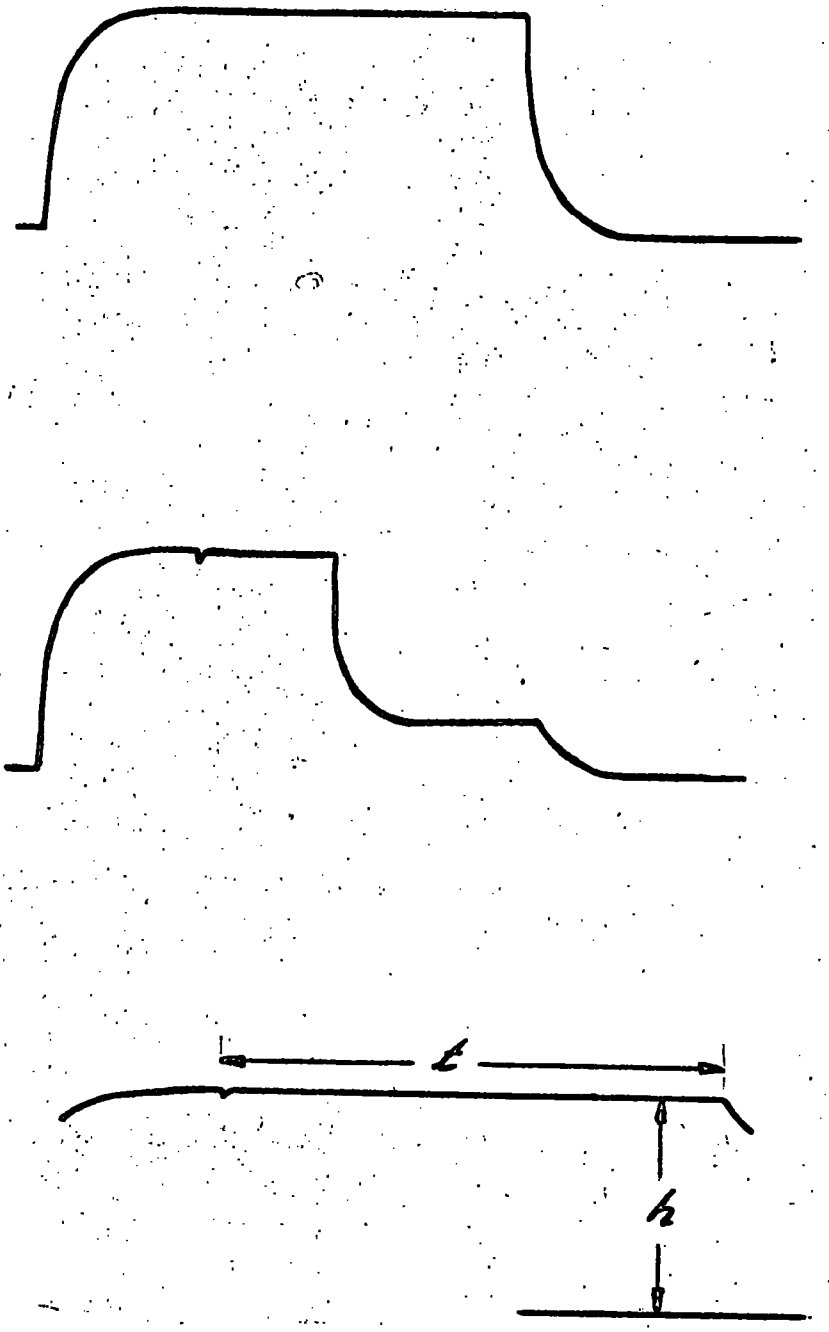

BREAKDOWN OSCILLOGRAMS.

fig 29

BREAKDOWN PROBABILITY

BREAKDOWN PROBABILITY

In order to determine the breakdown probability p, of a gap the number of observations which must be made to establish the probability and the error involved must be considered.

For a series of observations of the breakdown of a gap the mean probability is given by

$$\bar{p} = \sum_{s=1}^{n} f_s \cdot p_s \Big/ \sum_{s=1}^{n} f_s$$

and standard deviation

$$\sigma = \left[\Sigma (p_s - \bar{p})^2 / \Sigma f_s\right]^{\frac{1}{2}}$$

where fs is the frequency of an observation ps. For a normal or Gaussian distribution it can be shown that the probability that an observation lies between p_1 and p_2 is $\frac{1}{\sigma\sqrt{2\pi}} \int_{p_1}^{p_2} e^{-(p-\bar{p})^2/2\sigma^2} dp$

putting $(p-\bar{p})/\sigma = t$ this becomes

$$\frac{1}{\sqrt{2\pi}} \int_{p_1}^{p_2} e^{-\frac{1}{2}t^2} dt$$

It can therefore be expressed as the difference of two integrals of the type $\frac{1}{\sqrt{2\pi}} \int_{0}^{T} e^{-\frac{1}{2}t^2} dt$

These integrals are given in tables for various values of T. If this integral is evaluated between the limits -1 and +1 the value .68 is obtained showing that in any set of observations 68% will be expected to lie within σ of the mean.

Morse and Kimball show that if a determination of p is made it is possible to calculate a range of values of p within which it is 'reasonable' to find the true value of p. If for example we have m

successes in n trials the probability is m/n. By assuming various values of p it is possible to determine how reasonable they are from

$$G = \sqrt{\frac{2}{\pi}} \int_{\frac{m-np}{\sqrt{np(1-p)}}}^{\infty} e^{-\frac{1}{2}t^2} dt$$

G is the 'reasonableness' or 'goodness of fit'. The limit of reasonableness is usually taken as $G < .05$. Plots of G against assumed values of p are shown in fig. 30 for n = 100, m = 40 and n = 10, m = 4.

For $G < .05$ the values of p in the ranges .31 - .50 (n = 100) and .17 - .69 (n = 10) are reasonable.

Alternatively it can be decided what value of p is to be established and determine how many observations must be made to obtain an error of less than $\pm \eta$ with $G < .05$

$$G = \sqrt{\frac{2}{\pi}} \int_{x}^{\infty} e^{-\frac{1}{2}t^2} dt = F(\infty) - F(x)$$

where $F(\infty)$ and $F(x)$ are the values of the normal distribution function evaluated at ∞ and x respectively.

$$F(\infty) = 1$$

$$\therefore \quad F(x) = .95$$

from tables $x = 1.6$

Lewis shows that the number of pulses to be observed to establish a probability p with an error of $\pm \eta$ at a confidence level of .95 is given by

$$n = \frac{x^2 p(1-p)}{\eta^2}$$

A series of visual observations of the breakdown of air was made and the results compared with theory.

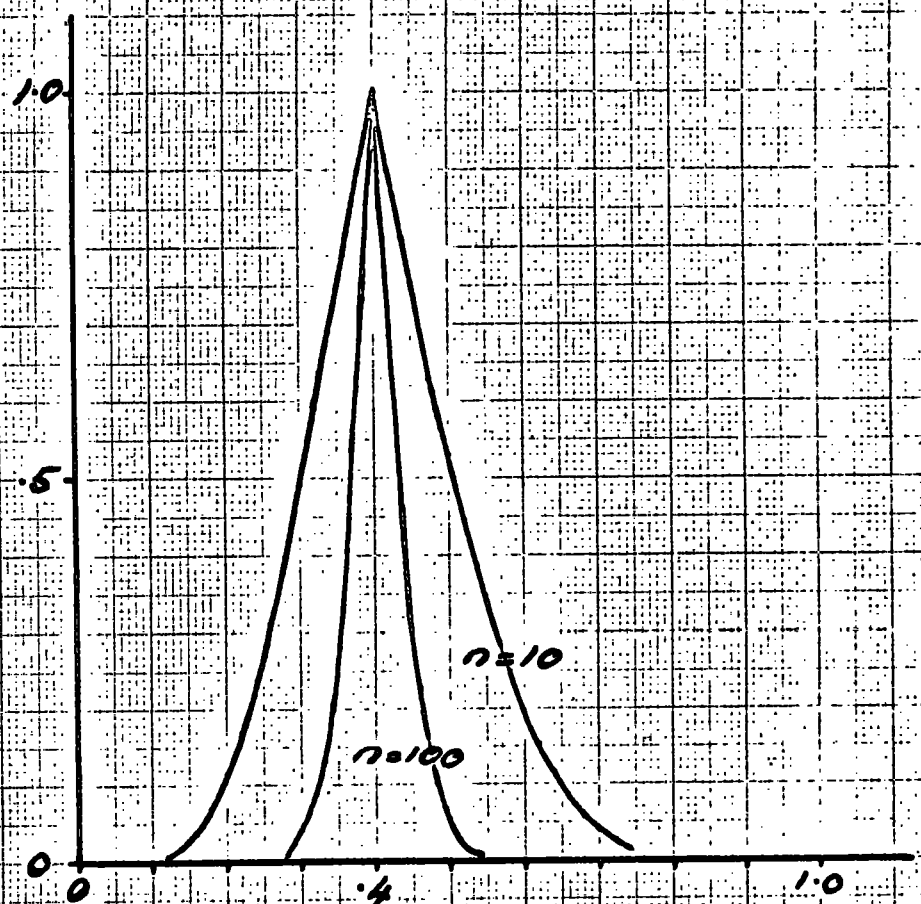

fig. 30

Total number of observations 1022

Total number of successes 86

Mean probability $\bar{p}$ = 86/1022 = 0.083

In fig. 31 is plotted breakdown probability as a function of number of trials. It can be seen that the mean value is not reached until approximately 800 trials but it is not necessary to observe as many as 800 to establish a breakdown probability of 0.08.

To establish the probability to within $\pm \eta$ the number of trials can be calculated from

$$n = \frac{x^2 \, p \, (1 - p)}{\eta^2}$$

for p = 0.083 $\eta = \pm 0.02$ n = 500

$\eta = \pm 0.03$ n = 230

Thus after 230 trials the value of the probability would be expected to lie within the range .11 - .05 and after 500 trials to lie within the range .10 - .06. These figures agree very well with the results shown in Fig.31.

The results were then divided into 10 groups of 100 and the mean and standard deviation calculated. These are tabulated below.

No. of successes in 100 trials	11	11	10	9	7	8	9	4	6	8
Breakdown probability	.11	.11	.10	.09	.07	.08	.09	.04	.06	.08
Deviation from mean	.03	.03	.03	.01	.01	.00	.01	.04	.02	.00

6 of these results lie within $\pm \sigma$ and 1 result lies at the limit of the goodness of fit (fig. 32) agreeing well with theory.

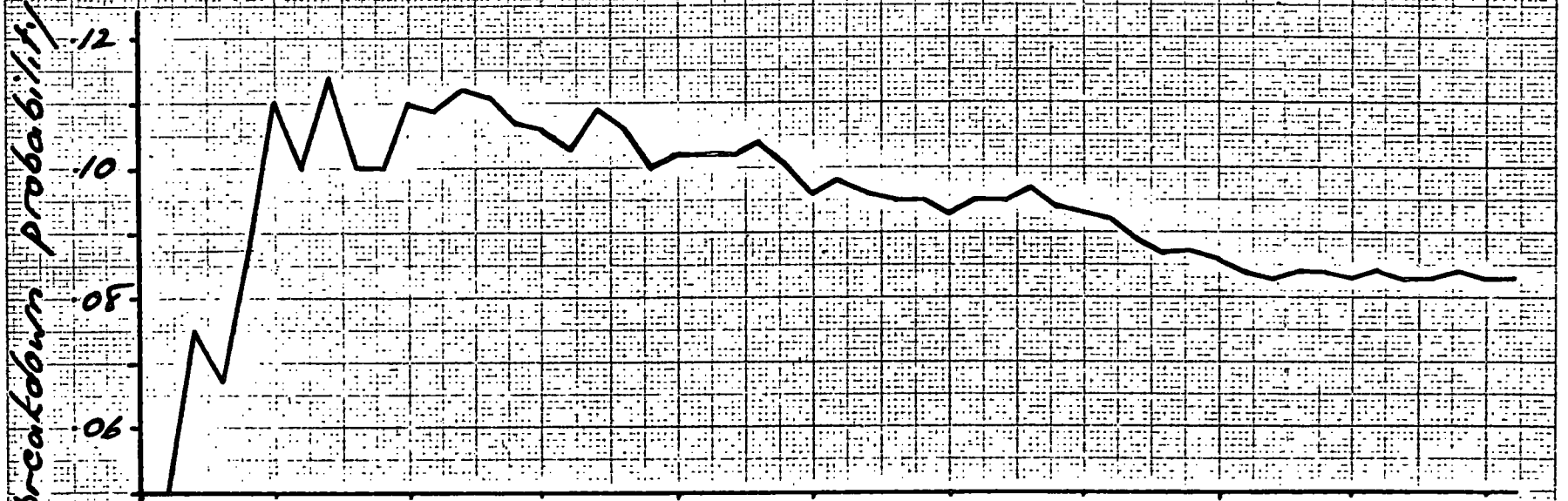

Fig. 31

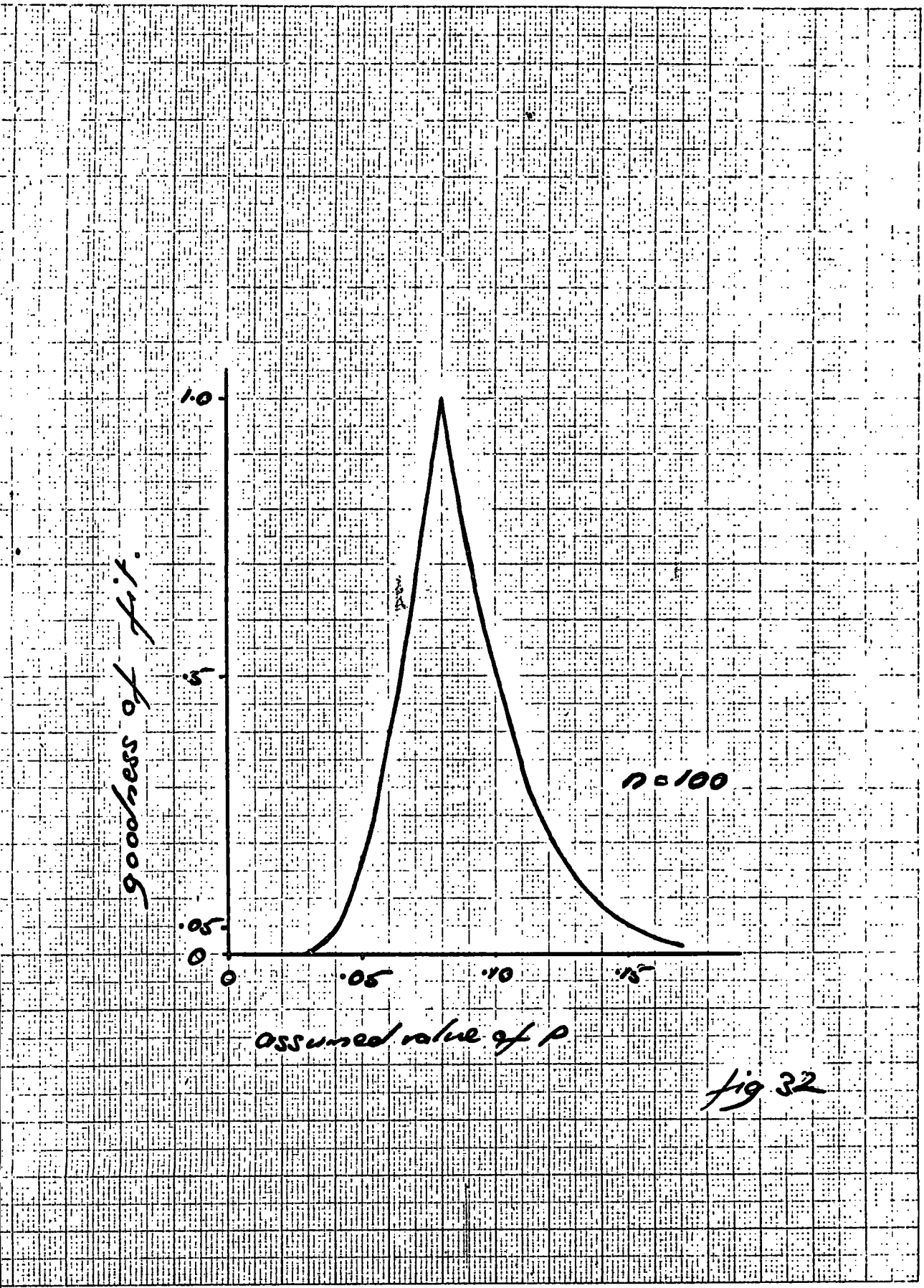

fig 32

When trying to establish the minimum breakdown potential it is not so much the value of the probability of breakdown under certain conditions that is important but whether the gap will break down at all. The question then arises, how many pulses must be observed before it can be decided that the gap will not break down?

The probability that the first breakdown in a sequence occurs in the m th trial is $p(1 - p)^{m-1}$ and the probability that a breakdown will not occur in the whole sequence is $(1 - p)^N$ where N is the total number of trials. This probability is shown as a function of N for various values of p in fig. 33.

For the set of 1022 pulses the following results are obtained of the number of groups having N pulses before breakdown for various values of N.

N	1	2	5	10	20	30	40	50	60
by calculation	7	6	16	19	22	9	4	1	0
by experiment	6	6	14	23	22	8	3	2	1

Observations were made of the variation of breakdown probability with applied voltage for various pressures in air and hydrogen. The criterion at this stage for the minimum breakdown was taken as no breakdown within 100 pulses. The breakdown voltage with sustained oscillations was also determined. These results are plotted in fig. 34. The points on the voltage axis refer to breakdown by sustained oscillations. It is seen that within experimental limits the minimum breakdown voltage for sustained and pulsed oscillations is the same.

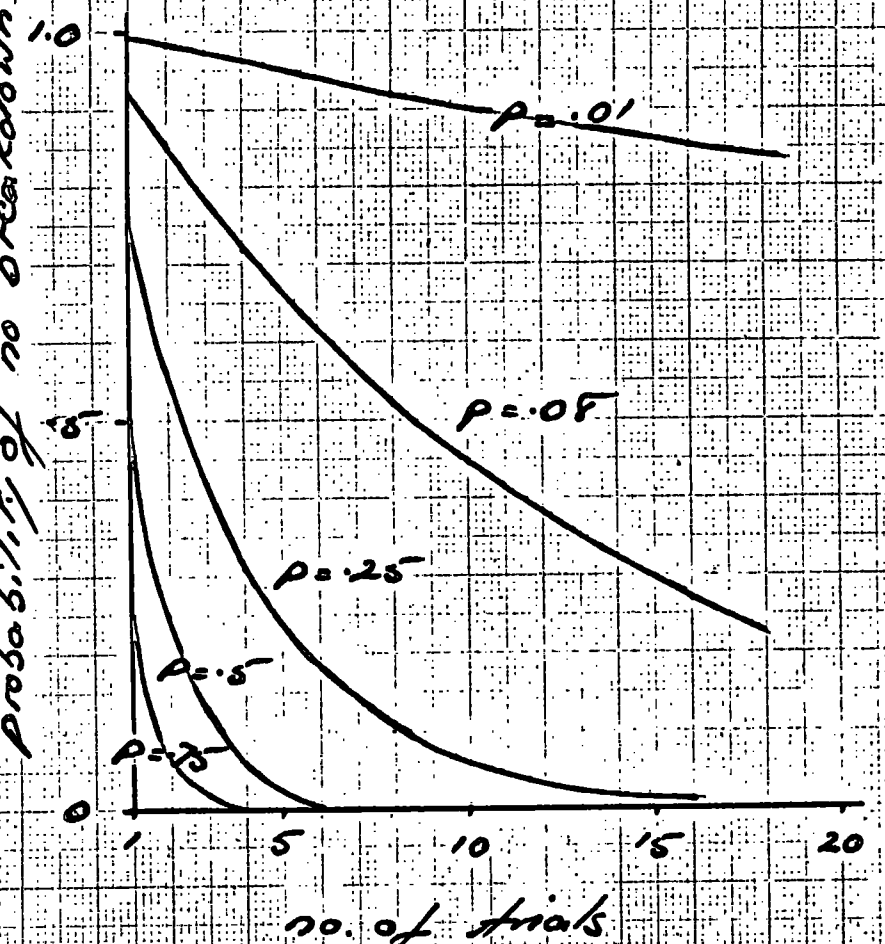
probability of no breakdown
1.0
.5
0
p=.01
p=.05
p=.25
p=.5
p=.75
1
5
10
15
20
no. of trials

fig 33

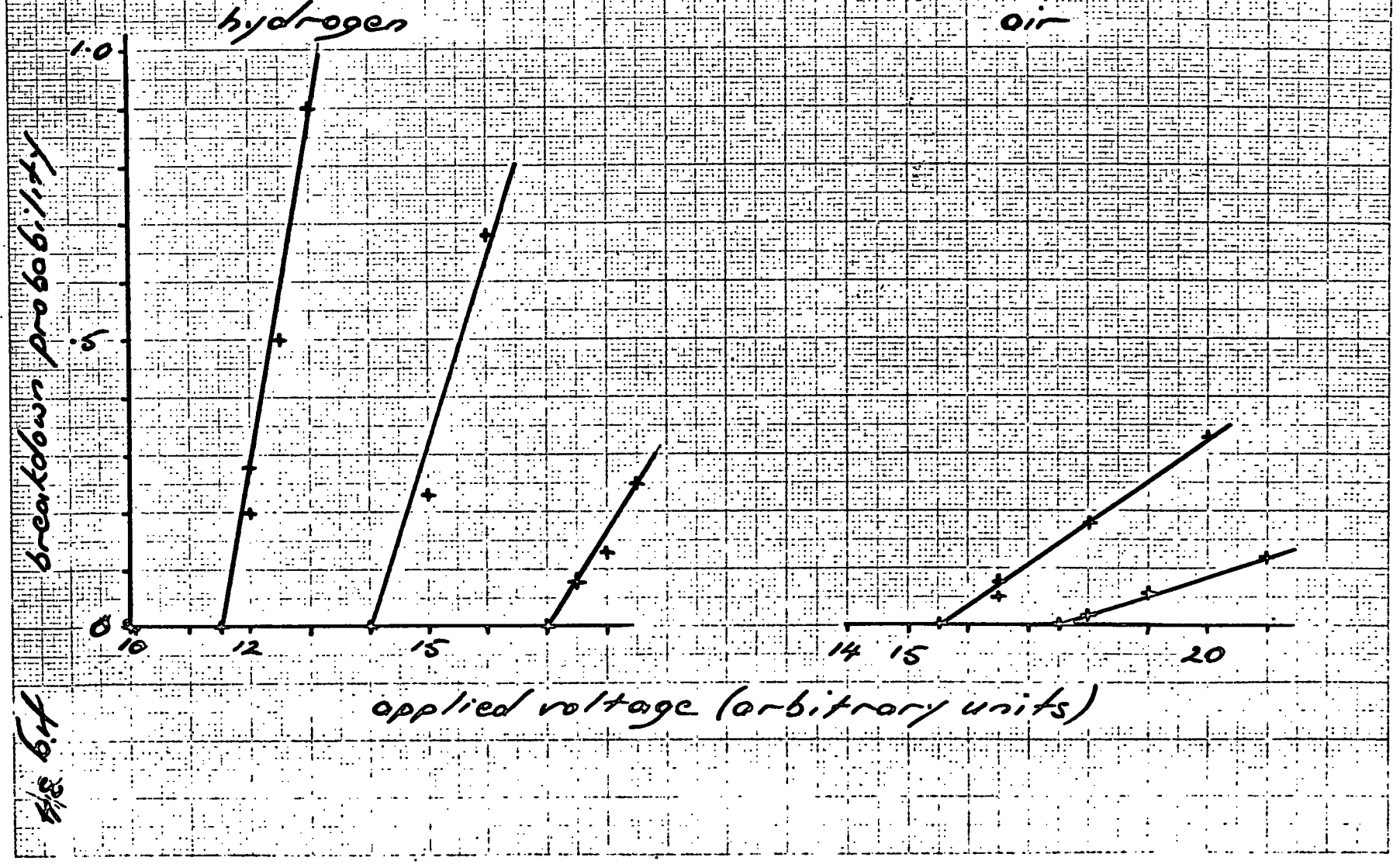
hydrogen
air
1.0
0
breakdown probability
10
12
15
14
15
20
applied voltage (arbitrary units)

Fig 8/4

The apparatus reproduces pulses with a variation in pulse height of approximately 5%. From the above results a 5% overvoltage corresponds approximately to a breakdown probability of 0.2. At a confidence level of 95%

$$(1 - p)^N > 0.05 \quad \text{for which} \quad N > 14$$

For air a 5% overvoltage corresponds to a breakdown probability of 0.05 for which $N > 59$. It would appear then that within the limits of the experiment 14 pulses in hydrogen and 59 pulses in air must be observed before it can be concluded that the gap will not break down.

To establish the minimum breakdown potential of any gas a rough breakdown probability-percentage overvoltage characteristic is obtained. The value of the probability to bring the value of the overvoltage to less than 5% is determined and this value is used to calculate the number of observations required at a confidence level of 95%.

VON LAUE PLOTS

VON LAUE PLOTS

~~The formative time tf is the least time interval between the application of the pulse and breakdown of the gap.~~

If the probability of breakdown per unit time is p, the breakdown in a short time interval dt is p.dt. The probability that no breakdown will occur during N successive time intervals dt is $(1 - p.dt)^N$

$$(1 - p.dt)^N = (1 + \frac{k}{N})^N$$

$$= \exp.k$$

$$= \exp.(-N.p.dt)$$

where $k = -N.p.dt$.

The probability $\underline{P}$ that breakdown will occur within a time N.dt of the application of the breakdown stress in thus

$$\underline{P} = 1 - \exp(-N.p.dt)$$

$$= 1 - \exp(-p.t)$$

where $t = N.dt$.

In any set of observations let

n_t = number of timelags of duration greater than t

n_o = number of applied pulses

then

$$\underline{P} = \frac{no - nt}{no}$$

$$= 1 - \frac{nt}{no}$$

hence

$$\frac{nt}{no} = \exp.(-pt)$$

or

$$\log(\frac{nt}{no}) = -p.t$$

The linear variation of log $(\frac{nt}{no})$ and t was first explained by von Laue and a plot of log $(\frac{nt}{no})$ as a function of t is known as a von Laue plot. The usual procedure is to express $\frac{nt}{no}$ as a percentage and to plot this on a logarithmic scale as a function of time on a linear scale.

The formative time tf is the least time interval between the application of the pulse and breakdown of the gap.

The statistical timelag ts is the arithmetic mean of all the timelags of the type t, and is equal to $^1/_p$

$$\log \frac{nt}{no} = -pt = -\frac{t}{ts}$$

so that when $\log (\frac{nt}{no}) = -1$, $t = ts$

$$\text{i.e.} \quad \frac{nt}{no} = e^{-1} = .368$$

If the results are plotted as indicated above the statistical time is given by the timelag corresponding to the ordinate 36.8%.

An analysis of a typical set of results is given below for one particular value of pulse height.

t = total timelag in microseconds, n = number of breakdowns in a time interval between t and $t + \Delta t$ where Δt is 10 microseconds. The results were taken in neon with a gap width of .5 cm and a pressure of 67 mm Hg.

t	n	n_t	$\frac{nt}{no}$ %
100	4	124	100
110	2	120	97
120	11	118	95
130	4	107	86
140	14	103	83
150	7	89	72
160	13	82	66
170	9	69	56
180	9	60	48
190	7	51	41
200	3	44	36
210	3	41	33
220	2	38	31
230	1	36	29
240	4	35	28
250	6	31	25
260	1	25	20
270	2	24	19
280	1	22	18
290	1	21	17
300	1	20	16
310	1	19	15
320	0	18	15
330	0	18	15
340	1	18	15
350	1	17	14
360	1	16	13
> 370	15	15	12

Referring to the table: there were no cases of breakdown showing a timelag less than 100μsec; there were 4 cases showing a timelag between 100 and 110μsec, 2 between 110 and 120μsec and so on. The total number of trials was 124, of which 120 showed a timelag greater than 110μsec, 118 greater than 120μsec and so on. These results are plotted in fig. 35 and the formative and statistical timelags indicated. These are 100μsec and 90μsec respectively.

The linearity of the von Laue plot may be interpreted in two ways. It may signify the probability of the arrival of a casual electron in the

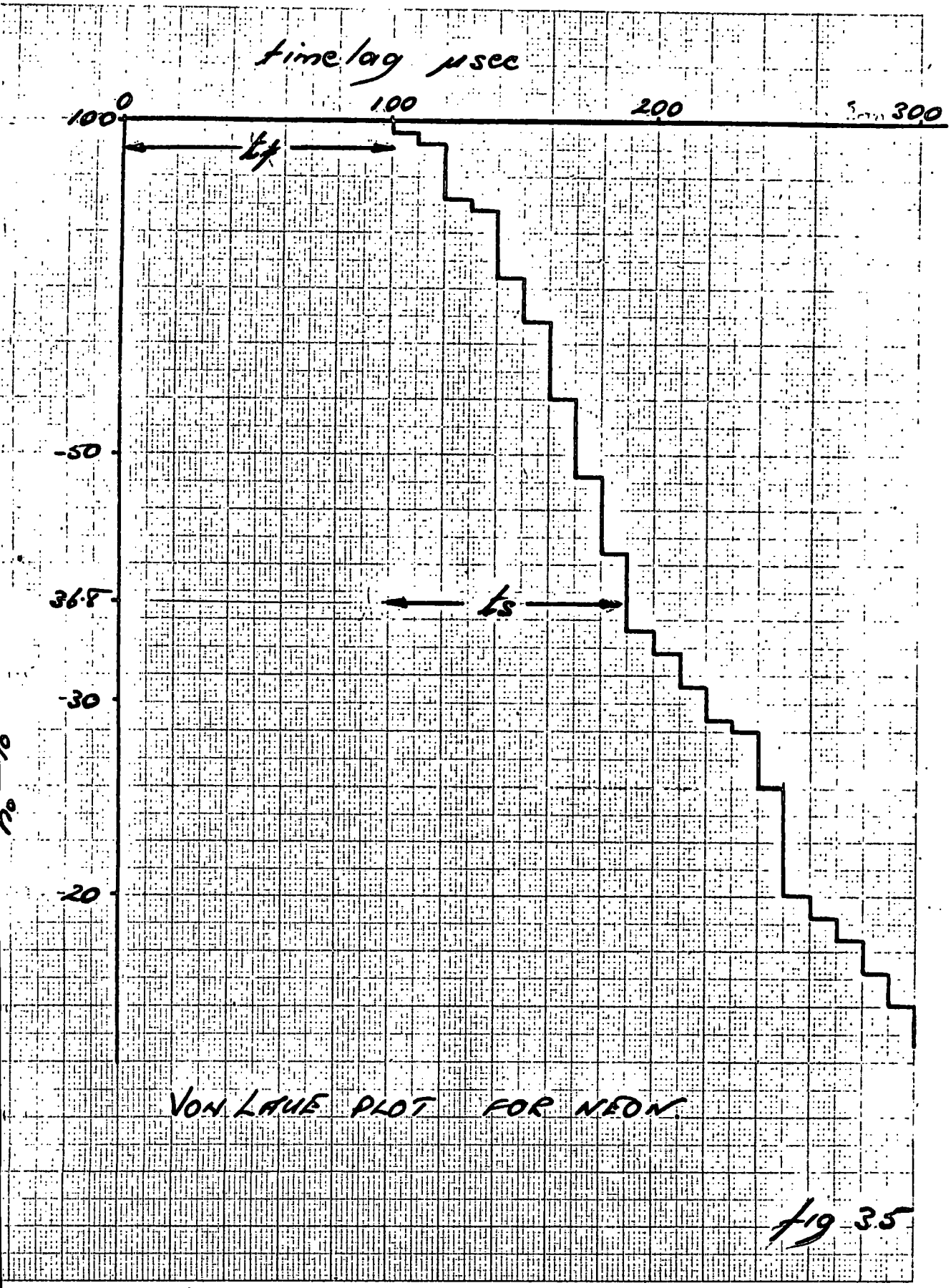

VON LAUE PLOT FOR NEON.

Fig 3.5

test gap, or the probability of the occurrence of a particular event leading to breakdown.

If it is assumed that breakdown occurs as a consequence of a number m, of ionizing events it can be shown mathematically that the von Laue plots will show considerable curvature towards the ordinate axis. Only when m = 1 is the von Laue plot strictly linear. If breakdown is to be preceded by more than a few ionizing events the von Laue plots show an appreciable apparent formative lag.

In fig. 36 are shown two of the plots recorded for air. It will be seen that these plots and the plots for neon are sensibly linear. In the example shown the formative timelag for air lies below the limit of resolution of the apparatus, i.e. is less than 10 microseconds and the statistical timelags are 15 and 353 microseconds.

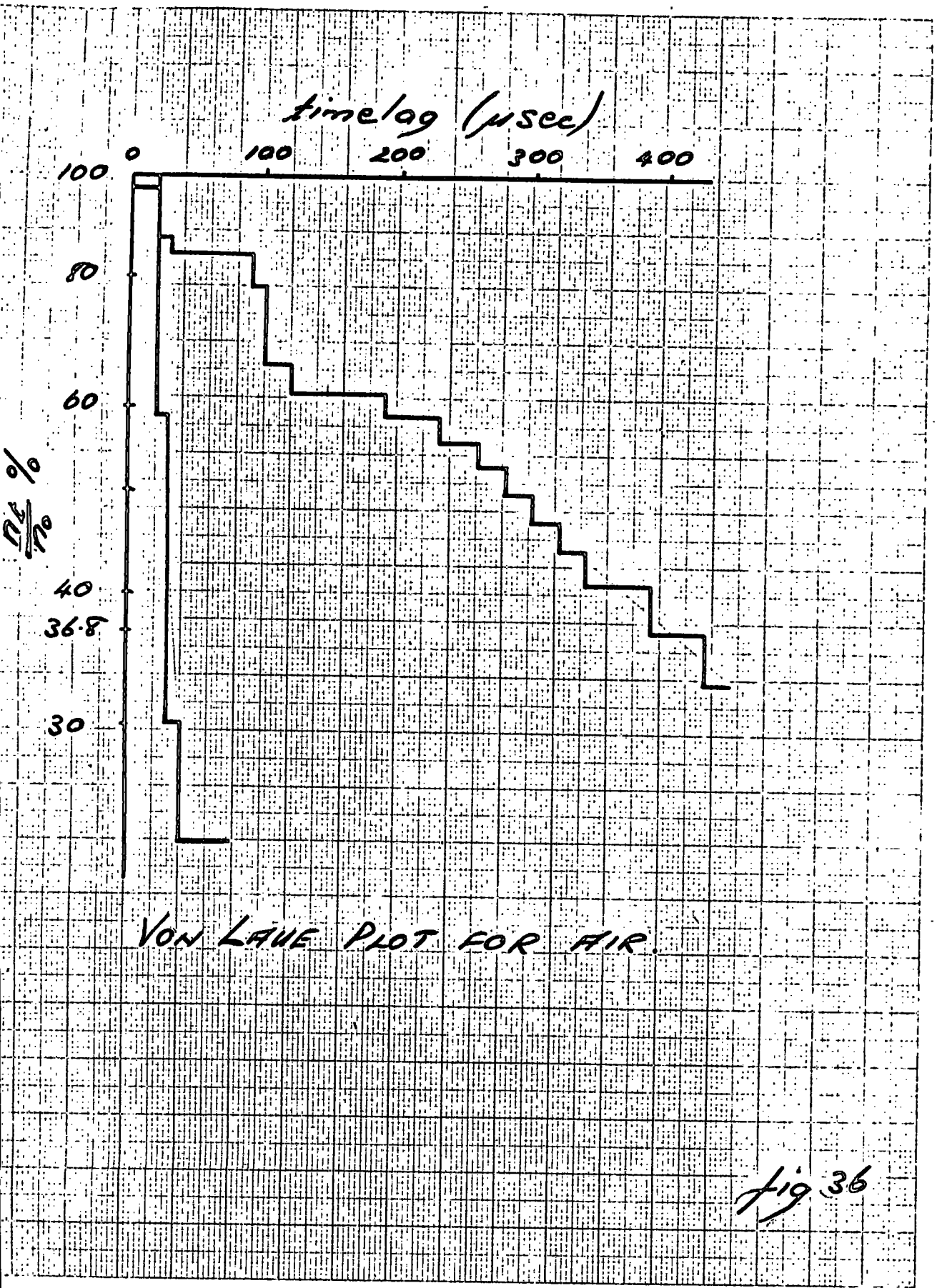

VON LAUE PLOT FOR AIR.

Fig 36

RESULTS OF BREAKDOWN TIME MEASUREMENTS

RESULTS OF BREAKDOWN TIME MEASUREMENTS

Measurements of the timelag to breakdown were taken for air, hydrogen and neon. These were carried out with various conditions of gap width and pressure.

Hydrogen

Observations were taken visually for gap widths of .25, .50 and .60 cm, and pressures in the range 1 to 20 mm Hg. In none of these conditions was it possible to detect any formative or statistical timelag.

The probability of breakdown was determined as a function of applied voltage. The minimum breakdown voltage was also determined for the same condition of gap width and gas pressure using continuous oscillations. The results show that the minimum breakdown is the same for pulsed and sustained oscillations.

Air

Visual observations showed that there was no formative lag but an appreciable statistical lag. A few von Laue plots were made from photographic observations.

Breakdown probability as a function of applied voltage was also determined.

Neon

Many results were taken for neon as this showed appreciable formative and statistical timelags. For a particular gap width and gas pressure a series of oscillograms were photographed for various values of applied voltage. Fig. 37 shows an analysis for results taken with a gap width of .5 cm and 11 mm Hg. The figures against the lines show, first applied voltage in arbitrary units and second (bracketed), the

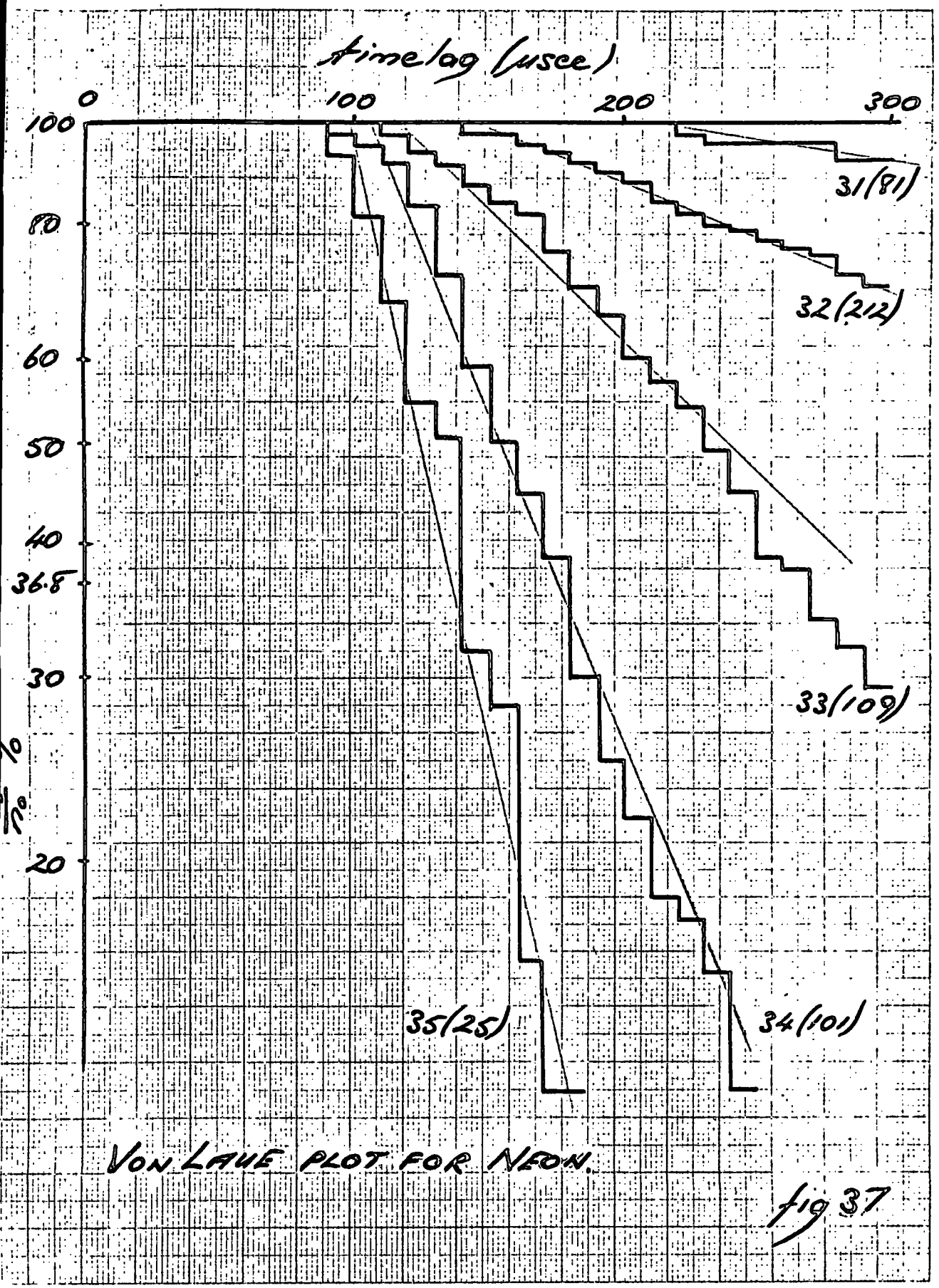

VON LAUE PLOT FOR NEON.

fig 37

the number of pulses making up the histogram.

The main results showing formative timelag as a function of breakdown stress are plotted in figures 38 and 39. It will be observed that:

(1) formative time and statistical time decrease with increase of applied voltage;

(2) breakdown stress increases with decrease in gap width;

(3) breakdown stress increases with increase in pressure.

Any theories which are put forward to explain the mechanism of u.h.f. gas breakdown under the conditions of this particular experiment must be consistent with these observations.

It was found that values of breakdown stress for particular values of formative time, gas pressure and gap width were reproducible to within approximately 10% of each other. These discrepancies are believed to be due to the influence of impurities in the gas specimen. A typical analysis of spectrally pure neon contains .1% of helium and impurities are liable to enter the system due to dry taps or inadequate outgassing before admitting the gas specimen.

The value of the minimum breakdown stress for sustained oscillations was also determined for various pressures and gap widths. It was found that for the same values of pressure and gap width the values of the breakdown stress for pulsed oscillations are asymptotic to the values obtained with sustained oscillations. The values obtained at 161 mm Hg are shown on fig. 38.

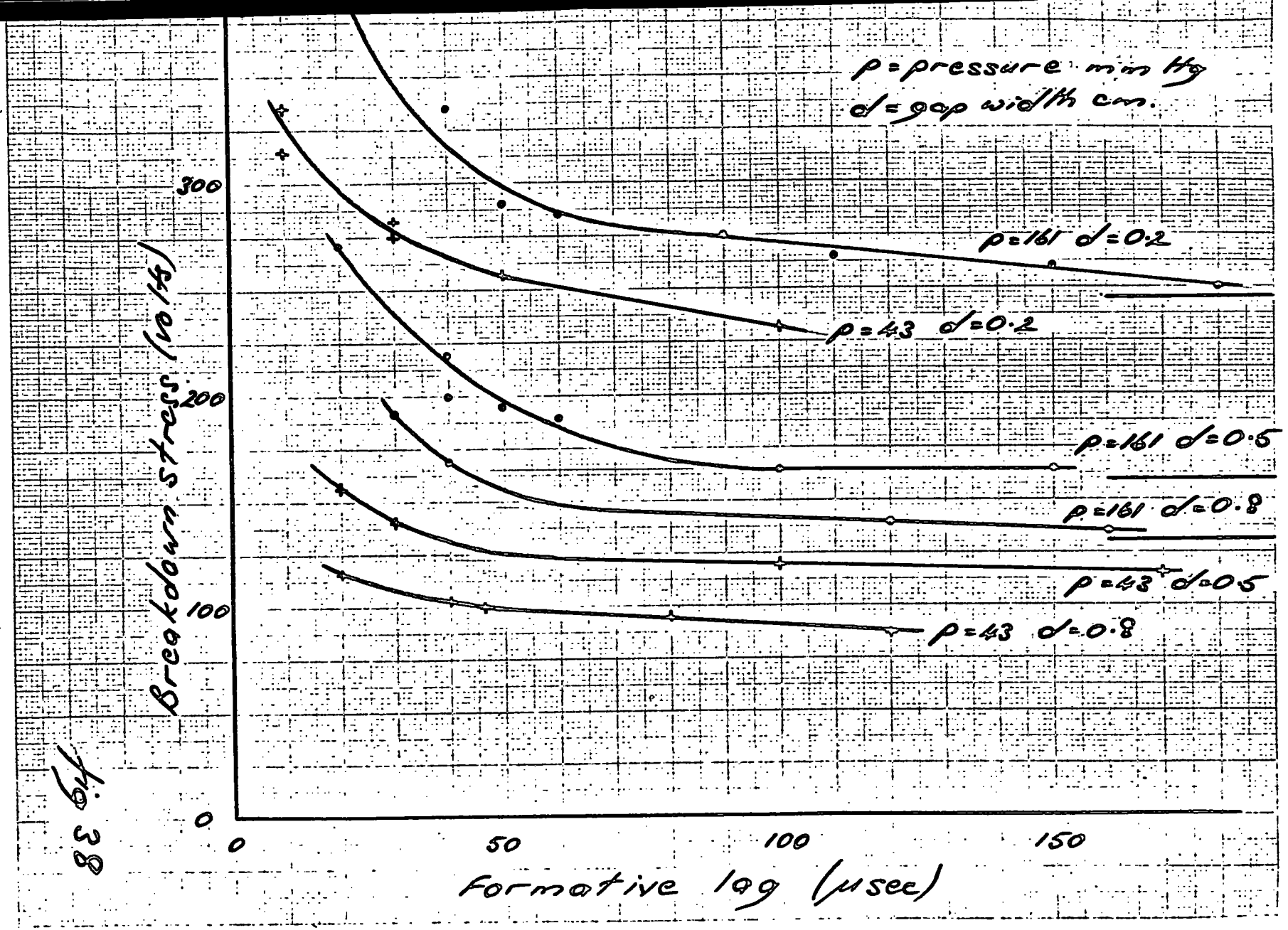
p = pressure mm Hg
d = gap width cm.
p=161 d=0.2
p=43 d=0.2
p=161 d=0.5
p=161 d=0.8
p=43 d=0.5
p=43 d=0.8
Breakdown stress (kv)
300
200
100
0
0
50
100
150
formative lag (μsec)

Fig. 38

Breakdown stress (volts)
200
100
0
0
50
100
Formative lag (μsec)
p=110 d=0.5
p=90
p=45 d=0.5
p=25 d=0.5

fig 39

DISCUSSION.

DISCUSSION

In order that breakdown shall occur in a finite time the rate of ionization must exceed that which is just sufficient to produce breakdown with sustained oscillations. Labrum has developed an expression for the time taken for an electron to reach a certain energy in a high frequency field.

If the number of electrons increases exponentially with time the number of electrons increases from n_o to n in a time t according to

$$n = n_o \text{ exp. } (G - L)\, t$$

where G is the number of ion pairs produced by an electron per second and L is the number that disappear per second.

If the criterion for breakdown is a certain number of electrons n_d in the gap then $(G - L)$ must exceed $\frac{1}{T} \log \left(\frac{n_d}{no}\right)$ for breakdown to occur where T is the duration of the applied pulse. Assume that each electron gains energy uniformly until its energy is slightly in excess of Vi the ionization potential of the molecule, produces an ion pair and then loses most of its energy. If it is also assumed that the loss of electrons is negligible during the period of the applied pulse so that L can be neglected this leads to an expression for breakdown in a field E of angular velocity w

$$E^2 \gg \frac{4\,Vi}{e/m} \quad \frac{w^2 + \frac{1}{3}\,vi^2}{vi} \quad \frac{1}{T} \quad \log \frac{n_d}{n_o}$$

where vi is the average collision frequency of an electron of energy Vi.

If Es is the minimum breakdown field for a pulse of duration T

$$T \propto \frac{1}{Es^2}$$

If at the beginning of the pulse there are n_o electrons in the gap the number of electrons after a time t will decay exponentially (fig. 40). If a field is applied to the gap the rate of decay of the number of electrons will be reduced. If Eo denotes the breakdown stress for sustained oscillations then the rate of electron production corresponding to Eo^2 is just sufficient to compensate for electron losses in the gap. If the field is greater than Eo then the electron population will grow until it reaches n_d when the gap will break down. In fig. 40 t_{f1} is the formative lag corresponding to an applied field E_1. Thus the rate at which the electron population grows is determined by $(Es^2 - Eo^2)$. In fig. 41 Es^2 is plotted as a function of $\frac{1}{tf}$ for the data shown in fig. 38. The graph is sensibly linear, suggesting that t_f represents the time taken for the electron population to reach a critical value.

There are various ways in which electrons can be lost from a gap. Prowse and Clark have shown that breakdown in neon in sustained oscillatory fields is a diffusion limited process. Brown et al. have developed the theory of microwave gas breakdown when the loss of electrons is by diffusion alone; the total flow of particles out of a volume of high concentration may be written as

$$\Gamma = - D.\nabla n$$

where Γ is the electron flow density in electrons per second per unit area, D is the diffusion coefficient for electrons and n the electron density. The continuity equation can be written as

$$\frac{\partial n}{\partial t} = vi.n - \nabla \Gamma$$

where vi is the frequency of ionization.

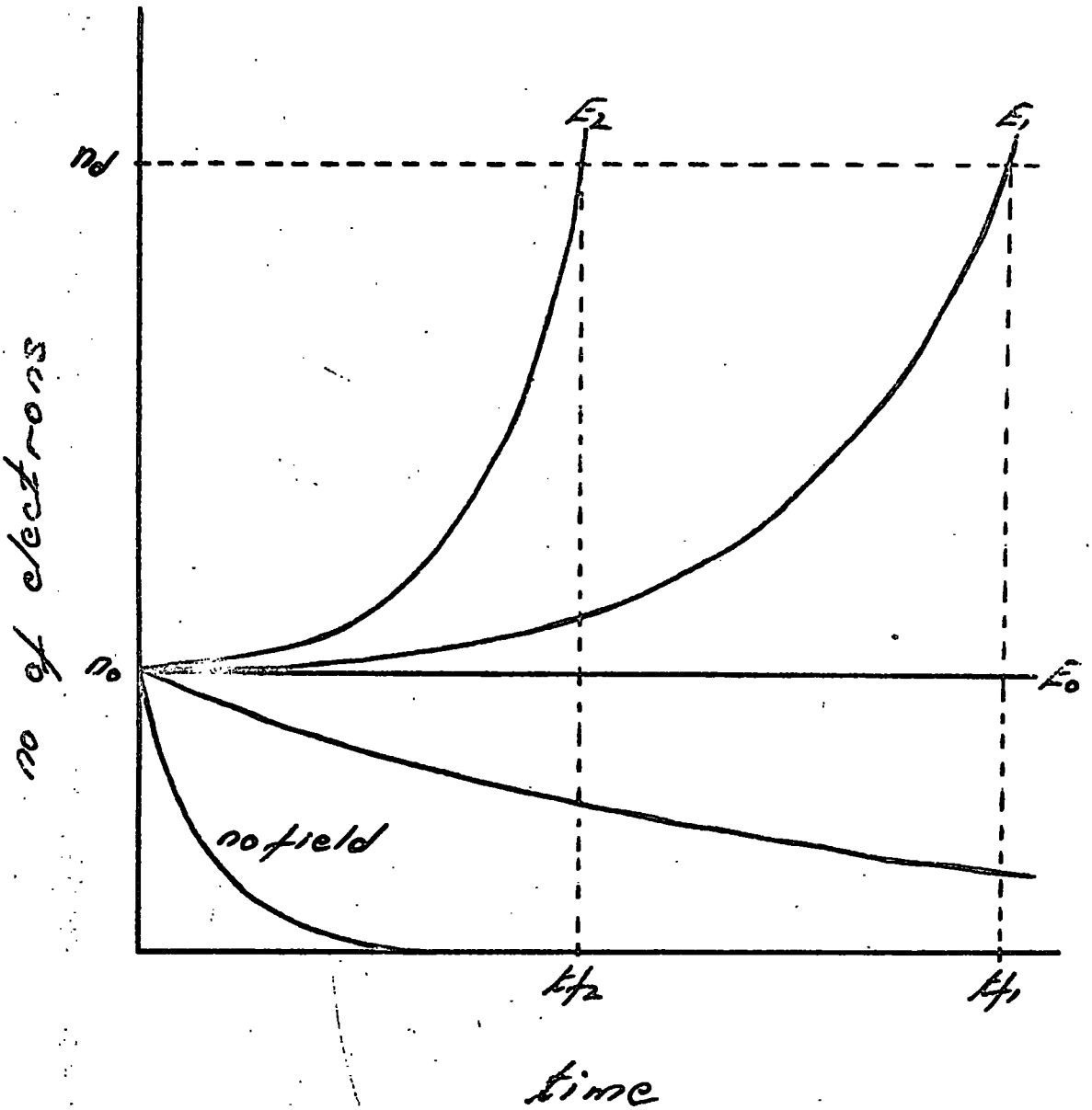

fig 40

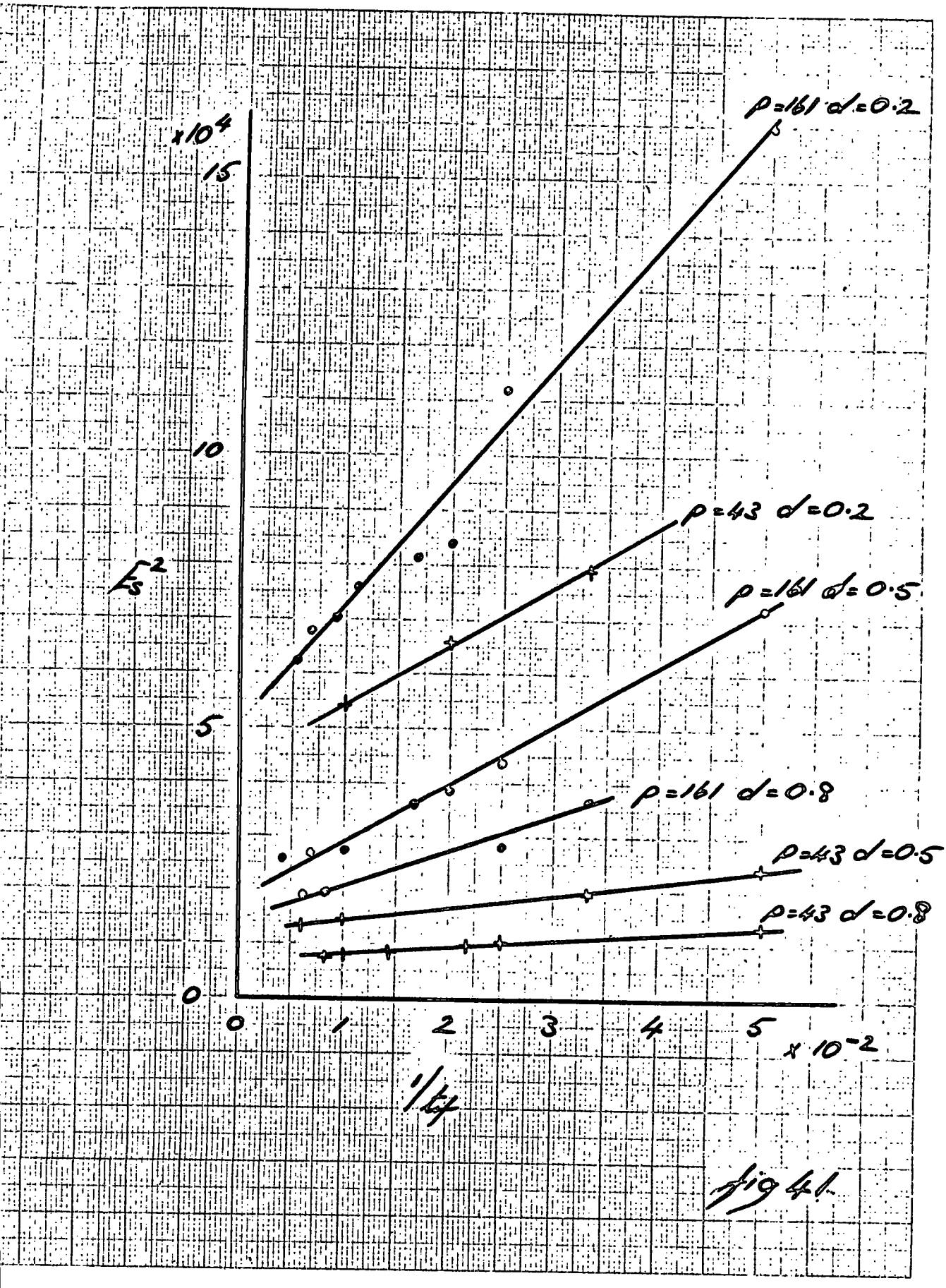
ρ=161 α=0.2
ρ=43 α=0.2
ρ=161 α=0.5
ρ=161 α=0.8
ρ=43 α=0.5
ρ=43 α=0.8
x10^4
15
10
5
0
F_s^2
0
1
2
3
4
5
x 10^-2
1/t_f

fig 41

These equations can be combined to give

$$\frac{\partial n}{\partial t} = vi.n + D.\nabla^2 n$$

$D.\nabla^2 n$ describes the loss of electrons by diffusion and $vi.n$ the gain of electrons by ionization.

Breakdown can be defined as the condition that the electron density goes to infinity. This occurs when $\frac{vi}{D} = \frac{1}{\Lambda^2}$ where Λ is known as the characteristic diffusion length. Λ is a very useful when describing the shape of the gas container when discussing diffusion problems. For a cylinder of length $\mathbf{1}$ and radius R

$$\frac{1}{\Lambda^2} = \left(\frac{\pi}{\mathbf{1}}\right)^2 + \left(\frac{2.405}{R}\right)^2$$

The first term on the right describes the diffusion to the end plates and the second term describes the diffusion to the cylindrical walls.

The mean lifetime t_d of a particle as limited by diffusion can be expressed in terms of the diffusion coefficient of the particle and the diffusion length of the gap:

$$t_d.D = \frac{\Lambda^2}{D}$$

The diffusion time (microseconds) of an electron in the test gap under typical conditions of pressure p and gap width d is given below.

p mm.Hg \ d cm.	0.2	0.5	0.8
161	0.07	0.44	1.14
11	0.005	0.03	0.08

As the breakdown time is longer than the diffusion time of an electron diffusion cannot be neglected as a removal mechanism.

Prowse and Jasinski measured formative timelags in neon in a cavity resonator with pulses of duration up to 2.5 microseconds. They found that (breakdown stress)$^{-2}$ was a linear function of pulse length. If the data in fig.38 are plotted in this way the plots are not linear (Fig. 42). Prowse and Jasinski used heavily overvolted gaps in their experiments and were able to neglect Eo^2. They were also able to neglect the effect of diffusion as the duration of the applied pulse was much shorter than the diffusion time of an electron in the test gap. In the present experiment diffusion cannot be neglected, nor can Eo^2 as the gap is not appreciably overvolted.

Reference to figs. 38 and 39 shows that the time scale varies comparatively little from curve to curve and that the variation is not obviously systematic. If diffusion were the controlling process then it would be expected that there would be a sharp dependence of time-constant on gap width.

It is recalled that an electron in an electric field gains energy until it is able to make exciting or ionizing collisions with the gas atoms. Two of the lower energy states of neon are metastable and the presence of metastable atoms is suggested as being of importance in the breakdown of neon in u.h.f. fields.

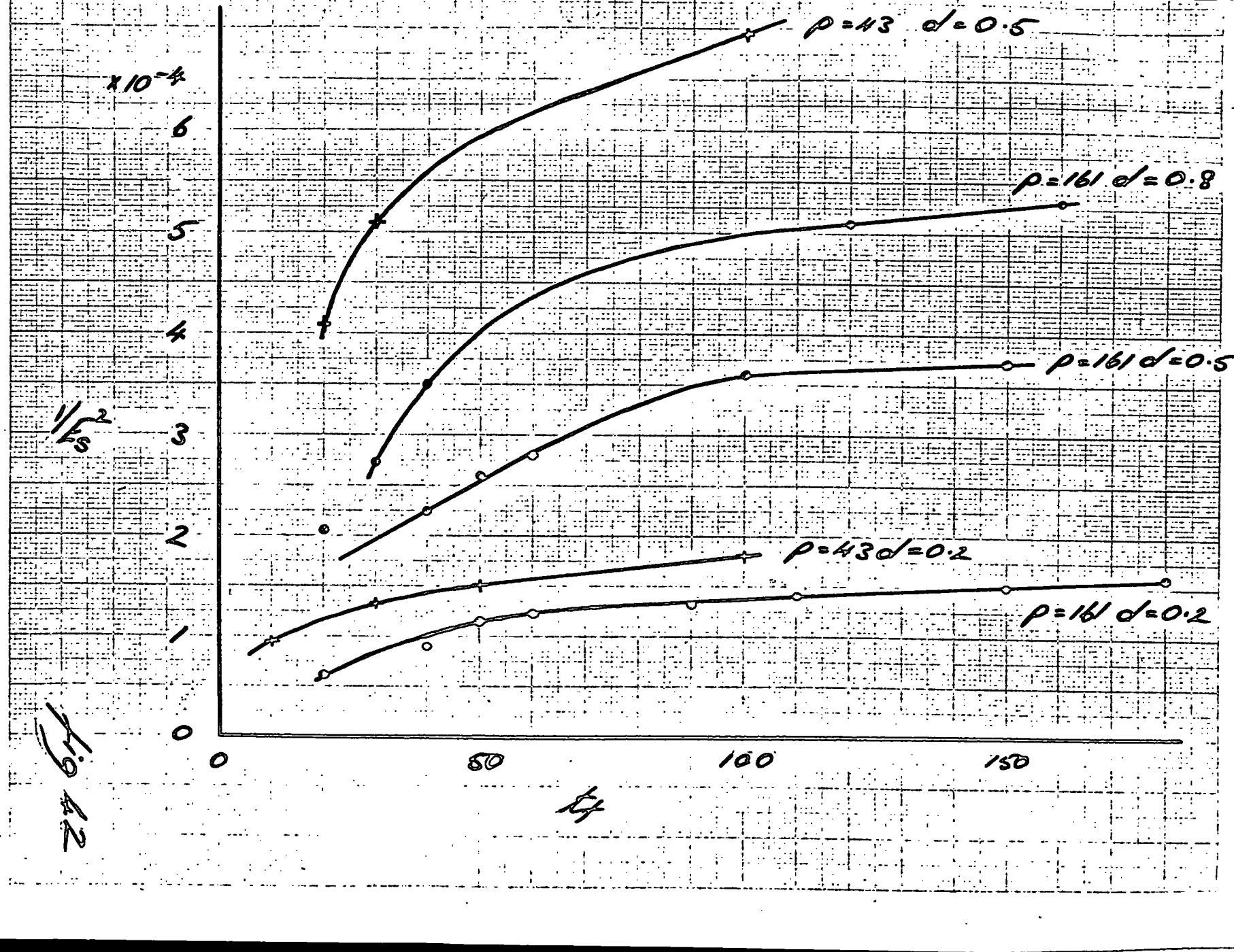
ρ=43 d=0.5
ρ=161 d=0.8
ρ=161 d=0.5
ρ=43 d=0.2
ρ=161 d=0.2
×10⁻⁴
6
5
4
3
2
1
0
1/L_s²
0
50
100
150
kμ

Fig. 12

METASTABLE STATES

METASTABLE STATES

There are at least four ways in which an atom in a metastable state can be changed into another state:

(1) It may receive sufficient energy by an impact with an electron to excite it to a still higher state. From the higher state transition to the normal state is possible.

(2) It may receive incident monochromatic radiation.

(3) It may be involved in a collision with another metastable atom resulting in the ionization of one of them and de-excitation of the other.

$$Ne^{*} + Ne^{*} \quad Ne^{+} + Ne + e$$

(4) If there is present an admixed gas whose ionization potential is lower than the excitation potential of the metastable state, the metastable atom may return to the normal state by ionizing one of the stranger atoms. (Penning effect)

The mean lifetime of a metastable atom a gas is determined by the various inelastic process listed above and by diffusion to the walls of the container. The Penning effect is an efficient process, particularly if argon is present as the energy levels of argon and neon are similar. The diffusion time (microseconds) of a metastable atom in the gap under typical conditions of the experiment is given below.

P mm Hg \ d cm	0.2	0.5	0.8
161	2.6×10^{3}	16×10^{3}	42×10^{3}
11	0.18×10^{3}	1.1×10^{3}	2.9×10^{3}

It is observed that the mean lifetime is comparable with or greater than the duration of the applied pulse.

Messner and Graffunder were the first to discover that illumination decreases the mean lifetime and concentration of metastable atoms. When an atom in a metastable state is illuminated by light of frequency v it absorbs energy E = hv (h is Planck's constant) and is raised to a higher excitation state. From this higher state the atom can readily return to the ground state.

BREAKDOWN OF ILLUMINATED GAP

BREAKDOWN OF ILLUMINATED GAP

A series of experiments was performed in which the test gap was illuminated by two small neon indicator tubes. The procedure was as follows:

The apparatus was allowed to run normally with a pulse rate of approximately one per second. The voltage across the test gap was adjusted to a value above the minimum breakdown value. By observing oscillograms of the voltage across the gap the breakdown probability was determined. The test gap was then illuminated with neon light. It was found that for approximately ten seconds after the commencement of illumination the gap continued to break down regularly but after this only seldom was a breakdown in the gap observed.

Some results are tabulated below. Ns is the number of breakdowns and No the total number of applied pulses in a given set of observations. The breakdown probability p, is the ratio Ns/No per cent. In the third column is given the number of breakdowns before the gap behaves regularly.

Dark gap		Irregular breakdowns	Illuminated gap	
Ns/No	P %		Ns/No	P %
35/37	95	5	0/12	0
29/30	97	5	0/18	0
28/28	100	4	0/22	0
18/18	100	8	1/34	3
41/56	73	0	0/31	0
Apparatus pumped out and refilled with fresh gas				
22/22	100	13	0/28	0
67/97	69	13	0/45	0
63/71	89	5	0/36	0
30/30	100	12	0/26	0
Break of approximately two hours				
32/32	100	7	1/22	5
33/33	100	5	0/37	0
28/28	100	14	0/24	0
32/34	94	12	0/31	0
Pulse height increased				
27/28	96	11	0/23	0
Pulse height increased				
13/13	100	28	3/22	14

The results indicate with very little doubt that metastable atoms play an important part in the breakdown process. When the test gap is initially illuminated it still contains metastable atoms from the previous breakdown and hence will continue to breakdown until the metastable atom concentration is reduced.

REFERENCES

REFERENCES

The following references have been quoted in the text:

Brode, Rev. Mod. Phys 5 257 (1933)

Herlin and Brown, Phys. Rev. 74 291 (1948)

Labrum, C.S.I.R., Australia R.P.R., 85 (1947)

Von Laue, Ann. Phys., Lpz, 76 261 (1925)

Lewis, Proc. Inst. E.E. pt C, 105 27 (1958)

Messner and Graffunder, Ann. Physik, 84 1009 (1927)

Morse and Kimball, Methods of Operations Research (1950)

Penning, Physica, 11 981 (1931)

Prowse and Clark, Proc. Phys. Soc., 72 625 (1958)

Prowse and Jasinski, Inst. E.E.Monograph 32 (1952)

Prowse and Lane, App. Sci. Res. B, 5 127 (1955)

The following references have been consulted and are relevant to the subject of the thesis:

Biondi	Phys. Rev. 82 453 (1951) Ionization by the collision of pairs of metastable atoms.
Biondi	Phys. Rev. 88 660 (1952) Diffusion, de-excitation and ionization cross-sections for metastable atoms.
Compton and Langmuir	Rev. Mod. Phys. 2 123 (1930) Electrical discharges in gases - survey of fundamental processes.
Dutton, Haydon and Llewellyn Jones	Brit. J. App. Phys. 4 170 (1953) Formative timelags in the electrical breakdown of gases.

Engstrom and Huxford	Phys. Rev. 58 67 (1940) Timelag analysis of the Townsend discharge in Argon.
Fisher and Benderson	Phys. Rev. 81 109 (1951) Formative timelags of spark breakdown in air in uniform fields at low overvoltages.
Gill and von Engel	Proc. Phys. Soc. 192 446 (1948) Starting potentials of high frequency gas discharges at low pressures.
Grant and Krumbein	Phys. Rev. 90 59 (1953) The effect of temperature on the duration of the $3P_2$ metastable level of neon.
Hale	Phys. Rev. 73 1046 (1948) The breakdown of gases in high frequency electrical fields.
Hartman	Phys. Rev. 73 316 (1948) Theory of high frequency gas discharges - high frequency breakdown.
Herlin and Brown	Phys. Rev. 74 291 (1948) Breakdown of gases at microwave frequencies.
Heymann	Proc. Phys. Soc. 63 B 25 (1950) Breakdown in cold cathode tubes at low pressures.
Loeb	Rev. Mod. Phys. 20 151 (1948) Statistical factors in spark discharge mechanisms.
MacDonald	Phys. Rev. 88 420 (1952) High frequency breakdown in neon.
MacDonald and Brown	Phys. Rev. 75 411 (1949) High frequency gas discharge breakdown in helium.
Meissner and Miller	Phys. Rev. 92 896 (1953) Influence of irradiation on the characteristic of glow discharge in pure rare gases.
Molnar	Phys. Rev. 83 933 (1951) Form of transient currents in Townsend discharges with metastables.
Morgan and Harcombe	Proc. Phys. Soc. 66 B 665 (1953) Fundamental processes of the initiation of electrical discharges.

Newton	Phys. Rev. 73 570 (1948) Transients in Townsend discharges.
Penning	Phil. Mag. 11 961 (1931) The starting potentials of the corona discharge in neon.
Pim	Proc. Inst. E.E. 96 pt.3 (1949) Electrical breakdown strength of air at u.h.f.
Posin	Phys. Rev. 73 796 (1948) The microwave spark.
Prowse and Cooper	Nature 161 310 (1948) Gas discharges at centimetre wavelengths.
Prowse and Jasinski	Nature 163 103 (1949) Oscillographic observations on ultra high frequency sparks.
Tillers	Phys. Rev. 46 1015 (1934) A survey of timelag of sparkover in a uniform field.
Townsend and Gill	Phil. Mag. 26 290 (1938) Generalization of the theory of electrical discharges.
Townsend and MacCallam	Phil. Mag. 6 857 (1928) Electrical properties of neon.
Wijsman	Phys. Rev. 75 833 (1949) Breakdown probability of a low pressure gas discharge.

REPRINT FROM PROCEEDINGS OF THE PHYSICAL SOCIETY

Reprinted from
Proceedings of the Physical Society, Vol. 79, Part 1, No. 507
1962
Printed in Great Britain by J. W. Arrowsmith Ltd., Bristol 3

Time Lags Associated with Ultra-high Frequency Gas Breakdown

By W. A. PROWSE, J. R. ROWBOTHAM and P. G. MONK

Department of Physics, Science Laboratories, University of Durham

MS. received 12*th February* 1961, *in revised form* 18*th July* 1961

Abstract. A method of measuring time lags associated with ultra-high frequency gas breakdown is based on the use of an oscillator giving a long pulse at 183 Mc/s. The time zero is fixed by the firing of an auxiliary spark which provides photo-electrons in the gas between the electrodes. Times-to-breakdown are then analysed into a statistical component t_s and a formative component t_f.

In hydrogen, gaps 0·25 cm to 0·60 cm (Rogowski electrodes) at pressures 1 to 20 mmHg were used. Visual examination showed no observable lag; i.e. the lowest field increase from condition of no breakdown moved the breakdown record to the time zero mark. In air for slightly shorter gaps there was no measurable formative time, but statistical lags up to hundreds of microseconds were observed.

In neon (0·2 to 0·8 cm gaps, pressures up to 161 mmHg) t_f and t_s were both measurable and were of comparable magnitude. The variation of t_f with applied field was not sensitive to gap width but could be explained by assuming that ionization in this gas was preceded by the formation of metastable atoms. Irradiating the gap with visible Ne light raised the breakdown potential.

§ 1. INTRODUCTION

The kind of breakdown considered is that which occurs when the frequency of the applied field is much below the electron collision frequency, but is yet so high that electrons in the gap are not swept by the field to the electrodes, but drift back and forth in the inter-electrode space. So far as sustained oscillations are concerned the mechanism of breakdown in these circumstances is well understood: in most cases the criterion for breakdown is that any electron in the field shall create at least one new electron by collision processes before random movement takes it out of the strong field region, i.e. breakdown is a matter of competition between collision ionization on the one hand and diffusion on the other (Brown 1956).

When pulses are employed the situation may be more complicated. It is evident that if the pulses are short enough the lifetime of an electron in the gap will be limited by the pulse duration instead of by diffusion, so that the minimum electric stress for breakdown must increase as the pulses are shortened. If a pulse of duration t_p and amplitude E_s can just break down the gas in the test gap, then when a sustained oscillatory field of amplitude E_s is applied instead the gap will not break down within a time t_p of the application. Thus t_p can be regarded as the formative time to breakdown for the stress E_s.

Experimental work on breakdown stress or on rate of growth of electron concentration as a function of pulse duration has been recorded by a number of authors (Posin 1948, Labrum 1947, Prowse and Jasinski 1952, Madan *et al.* 1957; also Francis and von Engel 1953 in a different range). Posin's measurements were made as utilitarian tests, but they include the interesting observation that a powerful radioactive source close to a given waveguide system would cause breakdown to occur at highly stressed

egions which otherwise did not show breakdown. It is not clear whether there was a owering of minimum breakdown stress or whether the radioactive source, by pre-onizing the gap, had made an otherwise rare event commonplace. Labrum found a ependence of breakdown stress on pulse duration in neon and concluded that his esults were consistent with the view that the growth of ionization during the pulse as limited by the pulse duration, not by electron removal processes. In air he found o dependence on pulse duration. Prowse and Jasinski measured relative breakdown tresses as a function of pulse duration for various gases in a cavity resonator energized 2800 Mc/s, using pulse durations from 0·25 μsec to 2·5 μsec. They found no depend-nce on pulse duration for the polyatomic gases they used but found a marked depend-nce in neon and some indication of dependence in argon and helium.

The present paper is concerned with an investigation of the time lags associated ith gas breakdown in correctly profiled parallel plate gaps (Prowse and Clark 1958) a frequency of 183 Mc/s.

§ 2. PRINCIPLES OF MEASUREMENT

Since no breakdown occurs until a time greater than the formative lag t_f has elapsed, e measurements may be made either by measuring breakdown probability P as a nction of pulse duration t_p or by obtaining oscillograms of the voltage across the ectrodes of the test gap as a function of time. The choice of method is much affected the nature of the statistical lag t_s.

Possibly the simplest conception of delay time is that which envisages a wait for e conditions prerequisite to breakdown (usually the appearance of a casual electron) llowed by the development to actual breakdown. If, out of n_0 trials each of duration n_f are failures, then the plot of $\log(n_f/n_0)$ as a function of t is linear (von Laue 1925) ovided the probability per second of the appearance of the casual electron is constant. n this plot t_f is the intercept; t_s is obtained from the slope (figure 5).

It is convenient to avoid the wait for the appearance of a casual electron by deliber-ely irradiating the gas between the electrodes, using a narrow pencil of ultra-violet diation produced by a small auxiliary spark in the same gas. This releases photo-ectrons in the gas (Prowse and Bainbridge 1957). A reference mark ($t=0$) is produced, by e discharge of the auxiliary spark, on the oscillogram used for display and measurement.

Assuming that at least one electron is present at $t = 0$, the growth of ionization is bject to statistical variations while the number of electrons is small, but as the number creases there is a change to a smooth progress (Prowse and Jasinski 1952).

When t_s is comparable with t_f it is advantageous to employ a pulse considerably nger than t_f and to observe the instant of breakdown rather than to employ pulses variable duration, because when the pulse duration does not much exceed t_f break-own becomes a rare event, whereas with the longer pulses breakdown is frequently bserved and each observation contributes to the determination of both t_f and t_s. The easurements on the oscillograms are grouped into time intervals so that the von aue plot is actually a histogram.

When t_f is small compared with t_s, visual observations can be advantageous. In e limiting case ($t_f \to 0$), the least observable increase in the applied potential causes change from no breakdown at all to breakdown with no observable formative lag. he qualitative observation is that in the latter case some traces show breakdown as ose to the mark of the irradiator spark as is observable.

If the idealized von Laue plot were linear and the formative lag were truly zero, en for $t_p = t_s$, P would be 36·8%. It is then easily shown that for $t_p = t_s \times 10^{-2}$,

P would be 1%. At this value, the probability of there being no breakdown in 10 trials is 45% and of there being no breakdown in 500 trials is 2%. Thus a few hundre visual observations could show that t_f is unlikely to exceed $t_s \times 10^{-2}$.

On the other hand, where t_f is comparable with t_s, the variation in t_f produced b voltage fluctuations within the accuracy of reading (some 2%) is usually much greate than $t_s \times 10^{-2}$. Thus an occasional visually unobservable fall in voltage could cause spurious early breakdown. The risk of error on this account is much reduced by using photographic recording.

§ 3. THE APPARATUS

A block diagram of the apparatus as a whole is given in figure 1 and some detail of the high-frequency arrangements are shown in figure 2.

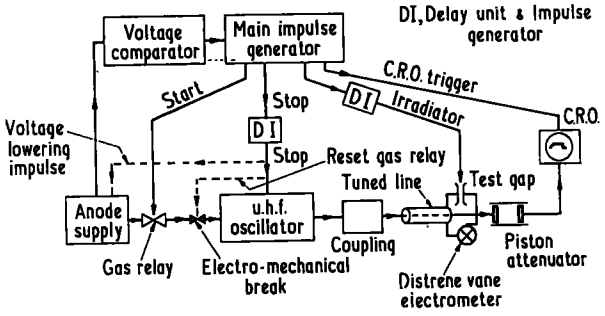

Figure 1. Block diagram of the apparatus. The train of events begins when the anode supply voltage reaches a preset value, causing the voltage comparator circuit to send a signal to the main impulse generator.

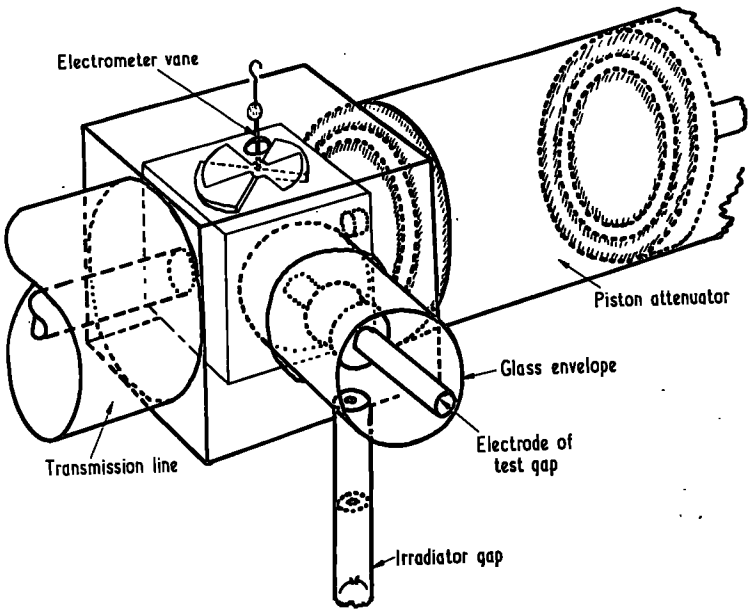

Figure 2. Sketch of the arrangements at the test-gap end of the transmission line, showing the electrometer, the piston attenuator and the general arrangement of the electrodes, but omitting the method of supporting the outer electrode and omitting the gas supply inlet and outlet.

The oscillator supplies energy to a coaxial transmission line some wavelengths ong by means of a tuned loop and sliding section. At the far end of the line the outer ube is expanded into a box and the inner supports a cube (figure 2) on which are nounted one of the electrodes of the spark gap, the raised quadrants of an electrometer nd the launching disk of a piston attenuator. Provision is made for calibrating the lectrometer using a low-frequency supply. The other electrode of the test gap is con- ected to the box through a flexible bellows (not shown) so that the gap length can be djusted and measured without interfering with the gas-tight envelope surrounding ne gap. A small auxiliary spark gap is mounted in a tube extending from the gas-tight nvelope and so arranged, with the aid of collimating disks, that a narrow pencil of adiation from the auxiliary gap passes through the centre of the test gap without ouching either electrode.

Behind the movable piston of the attenuator a diode and resistor are arranged so nat the envelope of the h.f. voltage across the test gap is displayed on the screen of cathode-ray tube.

Clearly, the timing of the auxiliary spark, the oscilloscope trace and the oscillator ulse are of considerable importance (figure 1). The immediate source of energy for ne oscillator, in pulsed working, is a bank of charged condensers and the system is o organized that when the potential of these reaches a preset value a voltage com- arator circuit comes into operation, producing a pulse which causes the main impulse enerator to fire. The pulse from this directly triggers the time base of the oscilloscope nd fires the gas relay tube which previously isolated the condenser bank from the scillator. It is also applied through delay circuits so as to produce the auxiliary spark r irradiating the test gap and to operate a circuit for stopping the oscillator, thus ontrolling the length of the high-frequency pulse. Expressed in terms of the oscillo- cope display, these events are shown in figure 3 which also shows the appearance of typical breakdown oscillogram.

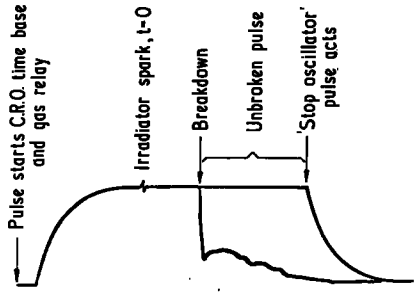

Figure 3. Diagram of a typical oscillogram, but showing an unbroken pulse superposed on a breakdown pulse and relating the features of the oscillogram to the functions of the circuits of figure 1.

A sharply resonant high frequency transmission line system is employed which has e advantage of discrimination against extraneous interference: it also allows a high oltage to be built up across the electrode system without an excessive energy input, that the spark gap and enclosure are readily cleared of discharge products after reakdown. Used in conjunction with a free-running oscillator the system is somewhat itical in adjustment. A concomitant of the sharp resonance is a relatively slow build-up

of oscillations on the line, making the beginning of the pulse difficult to define This was dealt with by using the firing of the auxiliary spark as a time zero mark.

It is very desirable that the flow of quite a small current in the test gap should produce a recognizable signal on the oscillogram, i.e. should produce a useful voltage drop at the electrodes, because only by this means would a gradual transition to conduction in the gas be revealed. The use of a high Q system is very suitable in this respect.

It was found in the first experiments with the system that breakdown was a very rare event unless an external source of electrons was provided. A radioactive source close to the gap made a considerable improvement, but the most satisfactory system was the use of the auxiliary spark to provide photoelectrons in mid-gap. A short length of wire on the input terminal of the oscilloscope readily picked up the sharp disturbance produced by the firing of the auxiliary spark, to give the time zero mark on the trace.

Provision was also made for the production of sustained oscillations, desirable as an extension to the measurements and essential for calibration. The oscillation amplitude permissible for pulse working was much higher than that permissible for sustained oscillations. Thus the principle adopted in calibration was to interpose a piston attenuator between the block and the oscilloscope, so that a calibration made with a sustained oscillation up to a voltage V could be used for pulsed voltages up to nV by setting the attenuator to apply the factor n. For this system to be satisfactory it was desirable that neither the voltmeter nor the attenuator should interfere with the working of the line.

A special electrometer was constructed (to be described more completely elsewhere) depending for its operation on the tractive force exerted on a slab of a dielectric medium in a stepped condenser, rather like a quadrant electrometer with a dielectric vane (Pim 1949). This could be calibrated at low frequency and used at any other frequency provided the change of permittivity with frequency is known. Polystyrene was used for which both the dielectric loss and the change of permittivity with frequency are small. A very satisfactory linear relation between deflection and (voltage)^2 was obtained.

The modes most generally employed in cylindrical piston attenuators are the dominant mode H_{11} and E_{01}. Of these H_{11} is the less attenuated but the launching device is a magnetic loop, i.e. of low impedance and unsuitable for the present purpose. But E_{01} is conveniently launched, and picked up, by means of a circular disk coaxial with the cylinder; this presents a high impedance load, predominantly capacitive. The final tuning of the transmission line, in use, is effected by a small trimming capacitor at the block and so the presence of a small capacitive load is unobjectionable. The H_{11} mode is axially asymmetrical and so any asymmetry in the elements of the piston attenuator is liable to couple the E_{01} mode to the H_{11} mode. Since the latter is less attenuated, precision of construction in the device is essential.

In practice, partly in order to avoid undue reliance on the constancy of the oscilloscope amplifier, the calibration was referred to the voltage level produced at the input to the oscilloscope; i.e. a set of unidirectional measured voltages was applied at the oscilloscope terminals and the attenuator was set so that the calibrating h.f. voltage produced a signal corresponding to a known voltage at the oscilloscope terminals. It was then easy to ensure that throughout the investigation the same portion of the diode characteristic was used.

Let V_1 and V_2 be the voltages developed between the pick-up disk and its surrounding ring for two settings of the piston, x_1 and x_2. Let λ and λ_c be the free spa

wavelength of the oscillation and the cut-off wavelength respectively. Then, for the E_{01} mode

$$\log \frac{V_1}{V_2} = \frac{1{\cdot}045}{r}\left(1-\frac{\lambda_c^2}{\lambda^2}\right)^{1/2}(z_1-z_2) \qquad (1)$$

where r is the inside radius of the cylinder. In the present experiments

$$(1-\lambda_c^2/\lambda^2)^{1/2} = 0{\cdot}992.$$

Equation (1) does not apply if the pick-up disk is so close to the launching disk that an appreciable amount of energy is reflected back to the launching disk. This is easily checked during calibration by verifying that a change in the piston attenuator setting does not affect the electrometer reading. Simultaneously it is easy to show that oscillation of the electrometer vane does not detune the transmission line, by verifying that the oscilloscope indication does not vary as the vane swings.

§ 4. EXPERIMENTAL RESULTS

All gases were commercial spectroscopically pure samples.

4.1. *Hydrogen*

Visual observations on breakdown in hydrogen were made for gaps of length 0·25 cm, 0·50 cm and 0·60 cm, and pressures in the range 1 to 20 mmHg. In every case the least alteration in field strength that could be used was sufficient to cause the change from no breakdown at all to breakdown with no significant lag, formative or statistical. It was verified from published data that only at the shortest gap and lowest pressure was the amplitude of electron drift movement comparable with the gap width.

The absence of formative lag in hydrogen was also examined by measuring P (the probability of breakdown) as a function of voltage for pulses of constant duration, and by measuring the breakdown voltage of the same gap for sustained oscillations ($t_p \to \infty$) (figure 4). It is seen that this latter voltage corresponds to $P \to 0$, i.e. that the minimum breakdown voltage for the pulse is identical with the minimum breakdown voltage for

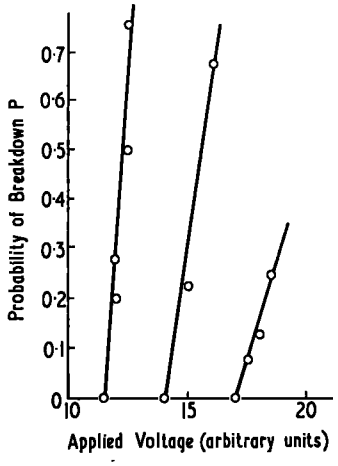

Figure 4. Probability of breakdown P as a function of applied voltage, for pulses of constant duration. Gas, hydrogen. The points on the voltage axis refer to breakdown by sustained oscillations.

sustained oscillations. The process is of some importance in that it eliminates th possibility of there being a very slow change of breakdown stress with pulse duratio for long pulses.

4.2. *Air*

Visual observations showed a complete absence of formative lag, as in hydroge but an appreciable statistical lag. In a few representative cases von Laue plots we made from photographed oscillograms and these all showed insignificant formati lags, but surprisingly long statistical lags. In the particular case of a gap of lengt 0·1 cm at a pressure 5 mmHg, the gap failed to break down at 120 volts applied; 133 volts it broke down showing zero formative lag and a statistical lag of 400 μse at 140 volts the statistical lag was 50 μsec. The times are approximate because the vo Laue plot was not straight, indicating that the probability of appearance of the triggerin event (e.g. appearance of a casual electron) was decreasing with time. Results f longer gaps were generally similar.

A similar examination to that made in hydrogen was also made in air, i.e. showin that the minimum breakdown voltage for a pulse of fixed duration is the same as t breakdown voltage for sustained oscillations. The least formative time that woul have been observable for air or hydrogen would have been about 10 μsec.

4.3. *Neon*

Preliminary visual observations showed that in neon the formative and the statistic lags were appreciable. Photographic records were therefore made and analysed provide von Laue plots (figure 5). In the typical experimental run shown in figu

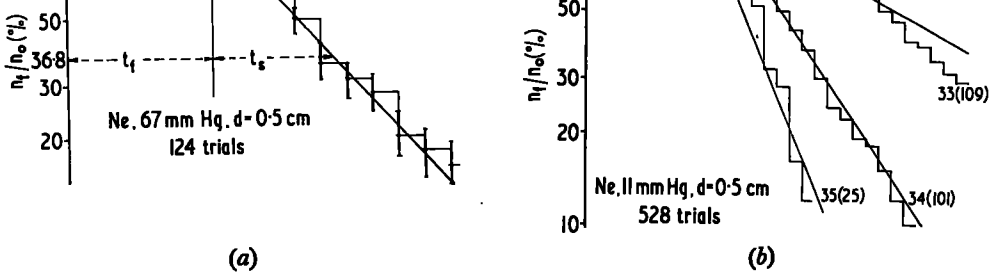

(*a*) (*b*)

Figure 5. Von Laue plots for neon. (*a*) Analysis of 124 applied pulses, showing the theoretical uncertainty in the values of n_t/n_0 (thick lines). (*b*) Analysis of 528 applied pulses. The figures against the lines show, first, applied voltage in arbitrary units; second (bracketed), the number of pulses making up the histogram.

5(*a*) 124 pulses were applied. At any given value of t, n_t represents the number pulses which had not, by this time, produced breakdown. Writing p for n_t/n_0 a q for $(1-n_t/n_0)$, the deviation for n_t may be written $\sigma_t = (n_0pq)^{1/2}$. In the figure t thick vertical lines show the range of values produced when n_t covers the range $n_t \pm$

Figure 5(*b*) refers to the analysis of a set of 528 trial pulses taken in conditions imperfect voltage stabilization. Here the records were first grouped according to pul height (in arbitrary units, pulse heights centred on 31, 32, 33, 34 and 35 were us

nd then sorted for the von Laue plots. It will be seen that not only the formative lag ut also the statistical lag decreases with increasing voltage. The tendency of the istograms to curve in towards the time axis cannot be relied on: pulses of the highest oltage in a group produce the earliest breakdowns and these are more conspicuous an the late breakdowns produced by the pulses of lower voltage. When the voltage abilization was more perfect this tendency to curvature became less evident.

It will be evident that more extended sets of results of the kind plotted in figure 5 ould provide histograms relating t_f and t_s to the applied voltage. Since the accuracy the voltage reading on the oscillograms is not considered better than 2%, the results btained with improved stabilization are not incomparably better than those obtained the method described. The chief results of this series of experiments are displayed figure 6. Gap lengths 0·2 cm, 0·5 cm and 0·8 cm were employed, and pressures in e range from 11 mmHg to 161 mmHg.

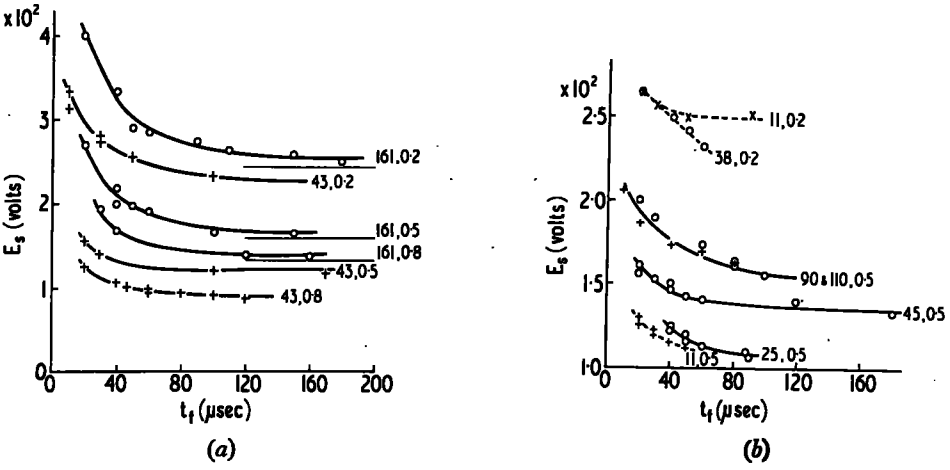

Figure 6. Formative lag t_f as a function of breakdown stress E_s for neon. On each curve the first figure is the pressure in mmHg, the second the gap width in cm. The asymptotes are measured values of breakdown by sustained oscillations.

In figure 6(*a*) the two sets of results were taken as one series without any change cept for the variation of gap length. The results shown in 6(*b*) relate to separate s fillings. For the curves shown dotted the amplitude of electron drift movement ceeded the gap width and they therefore are not comparable with the other results. so far as the curves may be loosely described in terms of a time constant, there is apparent alteration of this time constant within a set (figure 6(*a*)) despite the four- ld change of gap length. For one set, at 161 mmHg, breakdown observations were so made using sustained oscillations and these results are shown as asymptotes to e curves.

The lack of any obviously systematic variation of time constant (especially the sence of the sharp dependence on gap length characteristic of diffusion times) sug- sted that a process intrinsic to the gas was concerned. The possible importance of etastable atoms was therefore examined by investigating the effect of irradiating the test p with neon light through the glass envelope (Penning 1931).

A pulse of fixed duration was used and we observed the breakdown probability P ing at least 100 test pulses in each group, for the same gap with and without illumin- on by neon light (table 1). After a test with the dark gap there was always a period irregular behaviour before the neon light was fully effective: the corresponding

Table 1

Effect of Irradiating the Test Gap with Neon Light

P	dark gap (%)	95	97	100	100	73	41
n_2		5	5	4	8	0	
P	illuminated gap	0	0	0	3	0	
	Below, apparatus pumped out and refilled with fresh gas.						
P	dark gap (%)	100	69	89	100	100	100
n_2		13	13	5	12	7	5
P	illuminated gap	0	0	0	0	5	0

The first line gives the sparking probability P (per cent) without illumination; the second, the number n_2 of pulses during which the behaviour of the illuminated gap was irregular; the third, the sparking probability for the illuminated gap.

The pulse height was increased but no regular breakdown could be produced in the illuminated gap.

number of pulses n_2 is shown. At the end of the series of observations the pulse heigh was increased but no regular breakdown could be produced in the illuminated gap Thus the destruction of metastable atoms had prevented the development of ionizatio

A general correspondence (but not a strict proportionality) was observed betwee the values of the statistical and the formative lags in neon in reasonable accordanc with the suggestion that they represent two aspects of the growth of ionization from few initial electrons. A few observations were made on the relation between t_s an the flux of radiation from the auxiliary spark, by using two different sizes of the collim ating aperture. The results were consistent with an inverse proportionality betwee t_s and the flux of radiation.

§ 5. DISCUSSION

The experimental results on neon show that the form of the relation betwee formative time and the applied field is in qualitative accord with expectation inasmuc as increasing the field strength causes a decrease of formative time. But the gener time scale of the curves shows remarkably little variation with the experimental co ditions. In particular the values of the diffusion-limited lifetimes of electrons and metastable atoms appear to bear little relation to the time scale of the curves. For type of particle for which the coefficient of diffusion is D, the lifetime t_d is given by

$$t_d = \Lambda^2/D$$

where Λ is the diffusion length of the gap and may be written d/π for an ideal parall plate gap, i.e. neglecting lateral diffusion out of the gap.

For electrons $D = Wk/(40{\cdot}3E)$ where W is the drift velocity and k the ratio of t energy of an electron to that of a gas molecule in the field of strength E. This giv

$$t_d = 4{\cdot}08(E/p)(Wk)^{-1}pd^2.$$

Using Townsend's data, it is found that the value of $4{\cdot}08(E/p)(Wk)^{-1}$ does not va very much over the range of E/p employed, and t_d for neon may be calculated fr the relation

$$t_d = 1{\cdot}1 \times 10^{-8}pd^2.$$

Metastable atoms are assumed to resemble unexcited atoms, for diffusion calculations, and, in the table, gas-kinetic values have been used; i.e. $D = \eta'\rho$ where η' is the viscosity and ρ the density of the gas. This gives $D = 0{\cdot}328\ \text{cm}^2\ \text{sec}^{-1}$ for neon at 15 °C and 760 mm pressure, from which the diffusion limited lifetime of metastable atoms t_m is given by

$$t_m = 4{\cdot}07 \times 10^{-4} pd^2. \tag{3}$$

Table 2

Calculated Values for the Time required for Electrons t_e and for Metastable atoms t_m to Diffuse to the Electrodes

Neon

p = 161 mmHg			
d (cm)	0·2	0·5	0·8
t_e (μsec)	0·07	0·44	1·14
t_m (μsec)	$2{\cdot}6 \times 10^3$	16×10^3	42×10^3
p = 11 mmHg			
d (cm)	0·2	0·5	0·8
t_e (μsec)	0·005	0·03	0·08
t_m (μsec)	$1{\cdot}8 \times 10^2$	$1{\cdot}1 \times 10^3$	$2{\cdot}9 \times 10^3$

It is evident that t_e is much below and t_m much above the time characteristic of the experimental curves, and that the dependence of t_e and t_m on d is marked.

It is of interest to estimate the order of the number of electrons required to produce breakdown and to compare this with the number produced, in theory, by collision processes.

When ν electrons move with velocity W, the current flowing is $e\nu W$. This will suffice to remove the charge on the electrodes of the test gap in one cycle if

$$e\nu W = \omega CV \tag{4}$$

where C is the capacitance of the gap. From equation (4), $\nu = \omega A(4\pi em)^{-1}$ where A is the area of the electrodes and m the mobility of the electron, which is permissible when only rough values are sought. This number of electrons represents a maximum requirement. If the gap were in series with an inductance in a simple resonant circuit, a number of electrons νQ^{-1} would dissipate the energy as it arrived (Q being the quality factor of the circuit). In fact, the gap is a circuit element loading the end of a transmission line and it is suggested that a compromise value between ν and νQ^{-1} represents the situation. Since Q has a value of several thousand the number of electrons for breakdown is taken to be $\nu \times 10^{-2}$. This value is supported by another consideration. The test gap is the terminal load Z_T of a transmission line having a calculated impedance Z of 96 ohms. From equation (4), Z_T may be written $Ed(e\nu W)^{-1}$. When Z_T and Z are equal, the energy of the line is most rapidly dissipated in the gap. Writing ν_1 for the corresponding number of electrons, it is easily shown that $(\nu_1/\nu) = (\omega CZ)^{-1}$. For a gap of width 0·2 cm, this gives $\nu_1 = 0{\cdot}6 \times 10^{-2}\nu$.

The number of electrons so calculated is, for neon $0{\cdot}8 \times 10^9$, for hydrogen 3×10^9 and for air 2×10^9. It is now possible to see how these figures fit in with ionization

processes in neon. If N_0 electrons are present at $t = 0$, then the number N at tim t is given by

$$N/N_0 = \exp(\eta EWt) \qquad (5$$

where η is the ionizing efficiency, i.e. the number of ionizing collisions per volt dro in a unidirectional field. Kruithof and Penning's values of η are used (i) for Ne+ 3×10^{-5} A, (ii) for pure Ne. For breakdown starting from one electron,

$$\exp(\eta EWt) = 0{\cdot}8 \times 10^9, \quad \text{i.e.} \quad \eta EWt = 20.$$

Table 3

Electron Multiplication in Neon, for a 0·2 cm Gap and Pressure 161 mmHg

t (μsec)	40	60	90	150
E (v cm^{-1})	335	285	275	260
ηEWt (i)	710	770	1100	1600
ηEWt (ii)	12	11	13	18

The first two rows give the values of formative time and field-strength from the experimental curve, the other two rows the values of the exponent ηEWt, which theoretically should be 20 for breakdown; (i) Ne + 3×10^{-5} A (ii) pure Ne.

It appears that the electron multiplication to be expected in pure neon is somewha below that required, but that a very small argon content would be sufficient to increas the ionization rate enough to fit the experimental results.

§ 6. FORMATION AND STATISTICAL LAGS

6.1. *Neon*

No cases of breakdown were observed before the irradiating flash, so that th longest possible observed values of the statistical lag t_s should correspond to one electro present at the beginning. In this case the total number of electrons produced in time t (averaging a large number of trials) is $\exp(t/t_s)$. Thus when a time t_s elapses th number of electrons is multiplied by 2·7. Theoretically, 10^9 electrons are produce from one electron in an average time 20·8 t_s, or the formative time is about twenty time as long as the statistical lag. This is quite at variance with the experimental results i neon.

Prowse and Jasinski (1952) working with pulses so short that there was no time fo electron removal from the test gap found that (breakdown stress)$^{-2}$ was a linear functio of t in neon and explained this on the grounds that the rate at which an electron gain energy in a field of strength E varies as E^2. Extending this, in general terms, to th present case, let E_0 denote the breakdown stress for sustained oscillations; then th rate of electron production corresponding to E_0^2 just suffices to compensate for electro losses from the gap. Thus the rate at which electrons accumulate in the gap is deter mined by $(E_s^2 - E_0^2)$. In figure 7 Es^2 is plotted as a function of $1/t_f$ and the relatio is seen to be reasonably linear, agreeing with the suggestion that t_f represents the tim required for the electron concentration to reach a critical value.

The experimental results have shown that the formative times are not systematically ffected by pressure or gap lengths; that they are intermediate between diffusion mes for electrons and for metastable atoms; also that when metastable atoms are destroyed ie ionization is much reduced. Moreover earlier measurements (Prowse and Clark 958) have shown that breakdown in neon in sustained oscillatory fields is a diffusion-mited process.

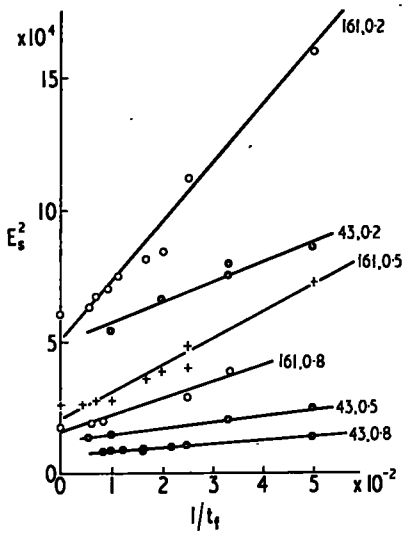

Figure 7. Relation between E_s^2 and $1/t_t$ for the data shown in figure 6(*a*). The data of the full curves of figure 6(*b*) give similar results.

It is therefore suggested, though with reserve, that the basis of the breakdown iechanism is the production of metastable atoms by electrons in the gap and the urther production of electrons by the metastable atoms in collisions of the second ind. The average metastable atom makes such a collision well within its diffusion-mited lifetime t_m and the build-up of metastable concentration is therefore not associ-ted with t_m. On the other hand the number of metastable atoms produced per electron is etermined by the lifetime of the electron t_e which agrees with the earlier measurements.

§ 7. BREAKDOWN IN AIR AND IN HYDROGEN

In order to estimate the diffusion times for electrons in hydrogen and in air the alues of $p\Lambda$ for various experimental conditions were calculated and the corresponding alues of $E\Lambda$ were ascertained from published data (Prowse and Clark 1958). Knowing E/p, we could then calculate the diffusion-limited lifetimes. For the longest gap 0·60 cm) and highest pressure (20 mmHg) used with hydrogen, the value of t_e so alculated was 1·2 microsecond; for the same conditions in air t_e was calculated to be ·94 microsecond. Thus the time range studied in the present experiments (> 10 μsec) epresents a large multiple of the diffusion-limited lifetime, and the apparent absence f formative lag is not in conflict with theory. It is however perhaps worth recalling hat in earlier microwave experiments the time range (0·25 μsec to 2·5 μsec) was much elow the diffusion times for the gap studied, but that here also no measurable formative ime was observed in air or hydrogen.

The experiments are being continued and it is hoped to cover the gap between he two types of condition.

ACKNOWLEDGMENTS

The authors wish to record their appreciation of generous and continued financi help from the British Electrical and Allied Industries Research Association, and t thank the Director of the Association for permission to publish this paper.

REFERENCES

BROWN, S. C., 1956, *Handb. d. Phys.*, Ed. S. Flügge, Vol. **22** (Berlin: Springer).
FRANCIS, G., and VON ENGEL, A., 1953, *Phil. Trans. Roy. Soc.*, A, **246**, 143.
KRUITHOF, A. A., and PENNING, F. M., 1937, *Physica, Haag*, **4**, 430.
LABRUM, N. R., 1947, *C.S.I.R. Australia RPR* 85.
VON LAUE, M., 1925, *Ann. Phys., Lpz.*, **76**, 261.
MADAN, M. P., GORDON, E. I., BUCHSBAUM, S. J., BROWN, S. C., 1957, *Phys. Rev.*, **106**, 839.
PENNING, F. M., 1931, *Physica*, **11**, 981.
PIM, J. A., 1949, *Proc. Instn Elect. Engrs*, III, **96**, 117.
POSIN, D. Q., 1948, *Phys. Rev.*, **73**, 496.
PROWSE, W. A., and BAINBRIDGE, G. R., 1957, *Canad. J. Phys.*, **35**, 324.
PROWSE, W. A., and CLARK, J. L., 1958, *Proc. Phys. Soc.*, **72**, 625.
PROWSE, W. A., and JASINSKI, W., 1952, *Instn Elect. Engrs Monograph* No. 32.

COMPLETE CIRCUIT DIAGRAM OF APPARATUS

Fig. 43 is a complete circuit diagram of the apparatus. The switch positions shown are for pulsed operation; when all the switches are in the other positions the apparatus will operate continuously. The letters a to h show the interconnection of the various units. For example the output of the multivibrator (marked b) is connected to the control grid of the main impulse generator when the apparatus is operating continuously.

VOLTAGE COMPARATOR

MAIN IMPULSE GENERATOR

ANODE SUPPLY FOR PULSED OSCILLATIONS

HT 1

240v ac

CRO sync

12v

240v ac

HT UNIT 3. 460v

VARIABLE DELAY (PULSE LENGTH)

IMPULSE GENERATOR (STOP)

OSCILLATOR

ANODE SUPPLY FOR CONTINUOUS OSCILLATIONS

HT 2

HT 3

CRO input